Induced polarization applied to biogeophysics: recent advances and future prospects

Kessouri[1,*] P., Furman[2] A., Huisman[3] J. A., Martin[4] T., Mellage[5] A., Ntarlagiannis[6] D., Bücker[7] M., Ehosioke[8] S., Fernandez[9] P., Flores-Orozco[10] A., Kemna[11] A., Nguyen[8] F., Pilawski[8] T., Saneiyan[6] S., Schmutz[12] M., Schwartz[13] N., Weigand[11] M., Wu[14] Y., Zhang[15] C., Placencia-Gomez[8] E.

[*] Corresponding author

[1] BRGM, French geological survey, 45060 Orléans, France, p.kessouri@brgm.fr (pauline.kessouri@gmail.com)

[2] Civil and Environmental Engineering Department, Technion, Technion city, Haifa 3200003, Israel,

[3] Agrosphere (IBG-3), Forschungszentrum Jülich GmbH, 52425 Jülich, Germany

[4] Lund University, John Ericssons väg 1, SE-22363 Lund, Sweden

[5] Center for Applied Geoscience, Hydrogeology, University of Tübingen, Hölderlinstraße 12, 72074 Tübingen, Germany

[6] Department of Earth and Environmental Sciences, Rutgers University – Newark, Smith Hall, Newark, NJ 07102, USA

[7] Institute for Geophysics and extraterrestrial Physics, TU Braunschweig, Mendelssohnstr. 3, 38106 Braunschweig, Germany

[8] Urban & Environmental Engineering, University of Liège, Quartier Polytech 1, Allée de la Découverte 9, 4000 Liège, Belgium

[9] Departement of Environmental Sciences, Norwegian University of Life Sciences, 1432 Ås, Norway

[10] Department of Geodesy and Geoinformation, Research Group Geophysics, TU Wien, Guhausstraße 27-29/E120, 1040 Vienna, Austria

[11] Geophysics Section, Institute of Geosciences, University of Bonn, Meckenheimer Allee 176, 53115 Bonn, Germany

[12] Bordeaux INP, Univ. Bordeaux Montaigne, G&E, EA 4592, F-33600, Pessac, France

[13] Robert H. Smith Faculty of Agriculture, Food and Environment, Dep. of Soil and Water Sciences, The Hebrew University of Jerusalem, 7610000, Rehovot, Israel

[14] Earth & Environmental Sciences Area, Lawrence Berkley National Laboratory (LBNL), Berkeley, CA 94720, USA

[15] Department of Geology, University of Kansas, Lawrence, KS 66045, USA

PostPrint for Self-archiving. Full publication is:

Kessouri, P., A. Furman, J.A. Huisman, T. Martin, A. Mellage, D. Ntarlagiannis, M. Bücker, S. Ehosioke, P. Fernandez, A. Flores-Orozco, A. Kemna, F. Nguyen, T. Pilawski, S. Saneiyan, M. Schmutz, N. Schwartz, M. Weigand, Y. Wu, C. Zhang, E. Placencia-Gomez. 2019. Induced polarization applied to biogeophysics: recent advances and future prospects. Near Surface Geophysics, 17(6), 595-621. doi: 10.1002/nsg.12072.

Acknowledgments

The motivation for this review resulted from the 5th International Workshop on Induced Polarization, which was held from October 3rd to 5th 2018 at Rutgers University-Newark, New Jersey (USA) and included biogeophysics as one of the five major topics. We acknowledge the members of the organizing and technical committees, the invited speaker on biogeophysical studies, S. Glaven, and all the participants of the workshop and especially of the biogeophysical studies roundtable for their fruitful discussions that helped shape this manuscript. We also thank Prof. Dr. Andrew Binley, Dr. Yves Robert Personna and an anonymous reviewer for their comments and suggestions that helped improve and clarify this manuscript.

Abstract

This paper provides an update on the fast-evolving field of the induced polarization (IP) method applied to biogeophysics. It emphasizes recent advances in the understanding of the IP signals stemming from biological materials and their activity, points out new developments and applications, and identifies existing knowledge gaps. The focus of this review is on the application of IP to study living organisms: soil micro-organisms and plants (both roots and stems). We first discuss observed links between the IP signal and microbial cell structure, activity and biofilm formation. We provide an up-to-date conceptual model of the electrical behavior of the microbial cells and biofilms under the influence of an external electrical field. We also review the latest biogeophysical studies, including work on hydrocarbon biodegradation, contaminant sequestration, soil strengthening and peatland characterization. We then elaborate on the IP signature of the plant root zone, relying on a conceptual model for the generation of biogeophysical signals from a plant root cell. First laboratory experiments show that single roots and root system are highly polarizable. They also present encouraging results for imaging root systems embedded in a medium, and gaining information on the mass density distribution, the structure or the physiological characteristics of root systems. In addition, we highlight the application of IP to characterize wood and tree structures through tomography of the stem. Finally, we discuss up- and down-scaling between laboratory and field studies, as well as joint interpretation of IP and other environmental data. We emphasize the need for intermediate scale studies and the benefits of using IP as a time-lapse monitoring method. We conclude with the promising integration of IP in interdisciplinary mechanistic models to better understand and quantify subsurface biogeochemical processes.

Key words: induced polarization, biogeophysics, complex conductivity, microbial cells, plants, trees

Introduction

In the past few decades, there has been an increasing recognition of the pivotal role of biological activity in subsurface processes (e.g. Konhauser 2007). Microorganisms play a crucial part in organic matter (OM) decomposition, precipitation/dissolution of minerals, and a multitude of other biogeochemical cycles (e.g. Mitsch and Gosselink 2015). Additionally, plant root systems can physically and chemically transform geological formations through cracks, water and nutrient uptake and storage (e.g. Tinker and Nye 2000). An improved understanding of the influence of the biosphere on subsurface processes is crucial in the coming years because it is linked with major economical, societal, and environmental challenges. For example, microorganisms are vital in the creation of wetlands that are important CO_2 sequestration pools (e.g. Lamers et al. 2012; Pester et al. 2012; Bodelier and Dedysh 2013); they contribute to soil quality through OM degradation (e.g. Fang et al. 2005; Lehmann and Kleber 2015; Parnas 1975); or play an important role in crop growth through their interaction with plant root systems (e.g. Avis et al. 2008; Grayston et al. 1997; Vacheron et al. 2013). Soil microorganisms can even be cultured for engineering applications, such as hydrocarbon degradation, contaminant sequestration or soil reinforcement (e.g. Atekwana et al. 2000; Colwell et al. 2005; DeJong et al. 2010). Apart from agricultural applications, understanding plant systems is also of interest, for example, for pollution monitoring and degradation (e.g. Salt et al. 1998; Pilon-Smits 2005;) and soil strengthening (e.g. Swanson and Dyrness 1975; Stokes et al. 2009; Ghestem et al. 2011).

Although the importance of the biosphere for physical and chemical transformations of geological media is widely acknowledged, the complexity of the induced changes remains hard to capture and explain. Soil or plant analyses classically used to study these processes involve sample excavation or trenching, are destructive and typically only provide a single snapshot in time (Atekwana and Slater 2009). Geophysical methods offer the advantage of being non-destructive, and have good spatial and temporal resolution. The study of the geophysical signature of biological processes in the subsurface is called biogeophysics. It is an interdisciplinary field at the border between geochemistry, microbiology, and geophysics. In its early stages, biogeophysical investigations were mainly focused on the geophysical signature of microbial cells, of dynamic microbial subsurface processes and of their

alteration of geological formations (Atekwana and Slater 2009). The first biological interpretation of geophysical signatures in the subsurface was proposed by Sauck et al. (1998), who observed conductive anomalies in sediments contaminated with petroleum hydrocarbons (also see Bermejo et al. 1997). This increase of electrical conductivity was attributed to an increase of ionic strength in groundwater created by weathering of sediments grains due to microbially mediated redox reactions producing CO_2 and organic acids. Besides, living cells themselves are polarizable – in particular in the low frequency range (below 100 Hz), as it has long been known from dielectric spectroscopy (e.g. Schwan, 1957; Fröhlich 1975; Foster and Schwan 1989; Prodan et al. 2004). Electrical impedance techniques are also routinely used in medicine and food industry as various cells exhibit characteristic spectral electric signatures (e.g. Holder 2004; Bera 2014; Barsoukov and Macdonald 2018). Recent developments (e.g. Vanderborght et al. 2013; Martin et al. 2012, 2015; Mary et al. 2017, 2018; Weigand and Kemna 2019) showed that geophysical methods are also sensitive to plant roots and processes associated with the development of plants and trees. We thus extend the definition of biogeophysics to also include the geophysical signature of plant root systems and trees. Among the existing geophysical methods, induced polarization (IP) is particularly well-suited to study biological processes in the subsurface, as it is sensitive not only to changes in the electrolyte chemistry through electrical conduction (charge transport), but also to changes at the surface of the mineral grains through electrical polarization (charge storage) (e.g. Binley and Kemna 2005; Slater and Atekwana 2009).

In a previous review of the field of biogeophysics, Atekwana and Slater (2009) illustrate the use of geophysical methods to detect byproducts of microbially mediated redox reactions (biomineralization of metallic iron minerals, calcium carbonate, and magnetic minerals) and point at the use of geophysical methods (magnetic and electromagnetic methods) to directly detect microbial cells and biofilms. In this review, we focus on the use of IP (spectral and time-domain) in recent biogeophysical studies. We provide an overview of the latest discoveries linking IP signals to subsurface microbial processes; and present new advances towards the characterization of plant root systems and trees using the IP method, which were not covered in Atekwana and Slater (2009). We also propose conceptual models explaining the polarization processes around a bacterial cell and the IP response of plant root systems, in

accordance with the latest mechanistic descriptions of cells and plant root polarization and empirical observations. Finally, we discuss challenges associated with the change of scales between laboratory results and field applications, and the joint interpretation of IP measurements with non-geophysical datasets.

Induced Polarization principles

IP is a geophysical method used to assess the electrical chargeability of the subsurface (i.e. its capacity to store charges) through the estimation of its complex conductivity σ^* or its reciprocal, the complex resistivity ρ^* (see Table 1). IP measures the low-frequency polarization (typically between 1 mHz and 10 kHz). It can be measured in the time domain and is then commonly referred to as time-domain IP (TDIP), or in the frequency domain and is then commonly called frequency-domain IP (FDIP) or, when screening a range of frequencies (commonly below 1 kHz), spectral IP (SIP). In TDIP, the secondary decay of the voltage is measured after the current shut-off, typically in form of the integral of the decay curve over predefined time windows (so-called integral chargeability), and the results are usually presented in terms of apparent chargeability. In FDIP, a phase-shifted voltage is measured relative to an injected alternating current. The results are expressed in terms of the amplitude and phase shift of the measured electrical impedance, which can be converted into real and imaginary conductivities - σ' and σ'' respectively, or magnitude and phase of the complex conductivity - $|\sigma^*|$ and φ respectively (see Table 1). Assuming a sufficiently high sampling rate of the decay curve of the TDIP measurements, very similar information can be extracted from FDIP and TDIP measurements, and even compared using the Fourier transform. A detailed review of IP methods can be found in, for example, Sumner (1976), Ward (1980), and Binley and Kemna (2005).

To analyze the spectral information contained in the IP data, several phenomenological models are used. The most popular ones are the Cole-Cole model (e.g. Cole and Cole 1941) and the Debye decomposition (e.g. Ustra et al. 2016). A comparison between the two approaches can be found for example in Weigand and Kemna (2016). The data can then be expressed in terms of: (i) a characteristic relaxation time τ_r

158 and an associated chargeability M_t ; or (ii) a distribution of relaxation times, each associated to a
159 chargeability value. These spectral parameters can in turn be related to different properties of the studied
160 biogeochemical processes.

161 In the field, the IP effect is generally represented as multi-dimensional maps of apparent or inverted
162 chargeability (usually for TDIP, but also for FDIP measurements), but can also be presented in terms
163 of frequency dependent resistivity, also called the PFE (Percent Frequency Effect), or as phase shifts in
164 FDIP. These measurements are equivalent, as they describe the ratio between polarizability and
165 conductivity of the studied formation (e.g. Slater and Lesmes 2002). Recent developments of the
166 method attempt to extract even more subsurface information, e.g., from the collection of full waveform
167 IP data (e.g. Fiandaca et al. 2012; Fiandaca et al. 2013), or the acquisition of spectral IP data using a
168 broad range of frequencies (e.g. Kemna et al. 2014; Kelter et al. 2018).

169

170 New insights on microbial cell polarization and their detection

171 Early biogeophysical applications of IP unequivocally highlighted the contribution of microbes to
172 subsurface charge storage (e.g. Atekwana et al. 2004b; Atekwana and Slater 2009; Ntarlagiannis and
173 Ferguson 2009; Zhang et al. 2014), or microbially mediated biogeochemical transformations (e.g. Slater
174 et al. 2007; Personna et al. 2008;). The role of microbes in modulating subsurface geo-electrical
175 properties was first highlighted at contaminated sites (e.g. Atekwana et al. 2004b; Abdel Aal et al.,
176 2004). Indeed, the attachment of cells onto mineral grain surfaces was postulated to increase surface
177 roughness, thus enhancing electrochemical polarization, while biofilms were thought to enhance
178 polarization and conduction pathways (Abdel Aal et al. 2004; 2009; Davis et al. 2006; Slater et al.
179 2007). In parallel, using dielectric spectroscopy methods, Prodan et al. (2004) detected low-frequency
180 (10 Hz) dielectric permittivity variations in *Escherichia coli* suspensions proportional to differences in
181 their abundance, thus highlighting the polarization effect of the microorganisms themselves. In
182 biogeophysics, it is only more recently that the contribution of the charged properties of cell membranes
183 and biofilms themselves to polarization was studied and even quantified (e.g. Revil et al. 2012 and

184 references therein). In the following subsections, we first describe the electrical behavior and
185 polarization of a microbial cell, before looking at the IP signature of biofilms and extracellular electron
186 transfer. We also discuss current state and future research direction to directly detect and characterize
187 microbial cells and biofilms using IP.

188 ***The bacterial cell structure and its electrical behavior***

189 Bacterial cells consist of a cytoplasm (a strong aqueous electrolyte exhibiting conductivities of up to
190 1 $S.m^{-1}$) encapsulated by a cell membrane (also called plasma membrane or cytoplasmic membrane),
191 surrounded by a cell wall (Parker et al., 2017, Willey et al. 2014). The outermost edge of the cell wall
192 can be conceptualized as a three-dimensional ion permeable shell made up of a network of polymers
193 (Carstensen and Marquis 1968; Poortinga et al. 2002; Sanchis et al. 2007; Revil et al. 2012). Thus, the
194 cell-surface resembles a polymeric brush layer which harbors carboxyl, phosphate and amino surface
195 groups and controls the cell surface charge (Revil et al., 2012). The enclosing cell membrane (Figure
196 1) prevents the flux of ions into the cell interior and can be considered an electrical insulator. Hence, as
197 an approximation, the bacterial cell can be considered as a non-conductive inorganic particle, (van der
198 Wal et al. 1997b). Two major groupings of bacteria emerge as function of the composition of their cell
199 wall: gram-positive and gram-negative. They are detected via the selective gram staining procedure
200 (Bartholomew and Mittwer, 1952). Specifically, gram-positive cell walls consist of a thick (from 20 to
201 80 nm) and homogeneous layer of peptidoglycan, surrounding the cytoplasmic membrane (Willey et
202 al. 2014). Molecules of teichoic and lipoteichoic acids are embedded into the peptidoglycan and extend
203 to the surface of the cell wall. Gram-negative cell walls have a much thinner peptidoglycan layer (from
204 2 to 7 nm), surrounded by a second lipid bilayer called the outer membrane (Willey et al., 2014). The
205 outer leaflet of the lipid bilayer contains lipopolysaccharides extending outward of the surface (Parker
206 et al. 2017, Willey et al. 2014). Despite these differences, the zeta potential of gram-positive and gram-
207 negative bacteria has been shown not to vary systematically (Poortinga et al., 2002; Baszkin and Norde,
208 1999). Thus, within the context of this review we have generalized the cell membrane model for both
209 types (Figure 1).

Protonation and deprotonation of functional groups within the polymeric brush layer result in the development of charges at bacterial surfaces (Carstensen and Marquis 1968; Poortinga et al. 2002; Claessens et al. 2004). Within the near-neutral pH range (pH 5-7), most gram-positive and gram-negative bacteria are net-negatively charged due to the higher proportion of carboxyl and phosphate groups with respect to amine groups, and their respective lower point of zero charge (Poortinga et al. 2002). The net-negative surface charge is neutralized by the electrostatic attraction of counterions, and their accumulation near the cell membrane surface, resulting in an electrical double layer (EDL). Unlike the EDL of mineral grains (very thin in comparison to the radius of curvature of the particle) (van der Wal et al. 1997a), the EDL of cells originates at, and within, the polymeric brush layer (Poortinga et al. 2002). The fixed negative charges are spatially distributed over the complete thickness of the polymeric brush layer, on the order of 10 nm (Figure 1b). High fixed charge densities within the ion penetrable cell surface, in conjunction with a high mobility of the corresponding counter-ions, yield a high surface conductivity of most bacterial cells.

Polarization of bacterial cells

Revil et al. (2012) developed a quantitative model to describe the induced polarization of bacteria, where Stern layer polarization and surface conduction within the polymeric brush (acting as a fixed-charge membrane at constant pH) drive significant charge storage (increase in σ'') at the outer-edge of cells. The Cole-Cole model (Cole and Cole 1941) was used to explain the low-frequency relaxation (1-100 Hz) associated with bacterial polarization, as a function of the ionic mobility within the cell EDL and the size of the polarizing cells (Revil et al., 2012). The modelling results of Revil et al. (2012) were supported by Zhang et al. (2014), who measured increasing frequency-dependent σ'' signals with increasing cell density of both, cell-suspensions and sand-cell mixtures of *Zymomonas mobilis*. Consistent, low-frequency σ''-peaks were measured around 0.1 and 10 Hz.

Furthermore, Mellage et al. (2018b) monitored the σ'' response of *Shewanella oneidensis* MR1 under growth conditions, in saturated quartz sand and iron-coated sand packed column-reactors. The proportional increase in σ'' with increasing biomass density further confirmed the direct dependence of σ'' on cell density. Mellage et al. (2018b) also extracted relaxation times (τ) from their measured spectra,

using the Cole-Cole model (σ'' spectral peaks between 5 and 40 Hz). Their relaxation times τ showed distinct variations as a function of the available electron accepting pathway in the column-reactors: (1) reduction of aqueous nitrate and nitrite, and (2) reduction of solid-phase ferric iron. The authors argue that τ can provide qualitative information relating to the size, activity and dynamic surface charging properties of the polarizing bacterial cells for spectra with well-defined peaks. The conceptualized Stern layer polarization of *S. oneidensis* is shown in Figure 2.

However, strict Stern layer polarization is not expected based on the structure of the outer cell-membrane. The polydisperse, permeable volume of the brush layer is in fact a three-dimensional distribution of charge (Poortinga et al. 2002; Revil et al. 2012). This is similar to the polydisperse polymeric coating on engineered nanoparticles, which deviates from the standard EDL model for non-permeable surfaces and exerts a strong control on electrochemical polarization (Mellage et al. 2018a). Polarization of coated nanoparticles deviates to a larger extent from the classical Stern layer model due to the much larger polydisperse volume in relation to the particle itself (Mellage et al. 2018a). Although a relatively thin layer in comparison to coated nanoparticles, polarization in the brush layer of bacterial cell membranes could, to some extent, also be controlled by charge accumulation within that layer. Incorporating elements from the NICA-Donnan model (Marinsky et al. 1983; Koopal et al. 1994; Benedetti et al. 1996; Kinniburgh et al. 1996), which accounts for the three-dimensional structure of soft polymeric substances, can be useful in improving our understanding and conceptualization of ionic migration along the surface of a bacterial cell, as has been postulated in Mellage et al. (2018a).

Biofilms

Biofilms are structured communities of cells enclosed in complex, hydrated (>80% water) organic structures attached to mineral and organic surfaces (Herbert-Guillou et al. 1999; Whitchurch et al. 2002; Kanematsu and Barry 2015; Berlanga and Guerrero 2016). The enclosing matrix is composed of diverse extracellular polymeric substances (EPS) such as polysaccharides, glycoproteins, lipopolysaccharides, uronic acids and extracellular DNA excreted by the bacteria (Poortinga et al. 2002; Whitchurch et al. 2002). The ions and nutrients transported in the aqueous biofilm phase make biofilms excellent ionic conductors (Malvankar et al. 2012; Beyenal and Babauta 2015). Potassium ion-channel based electrical

signaling within biofilms can attract distant cells (Humphries et al. 2017), and biofilm matrices can also include noncellular materials, such as minerals, clay or silt particles, depending on their external environment (Donlan, 2002), which contribute to enhanced surface conduction pathways. Furthermore, EPS might display semi-conductive properties once hydrated or ionized and behave like polymer electrolytes or conductive polymers (Borole et al. 2011). However, the electrical conductivity of biofilms has never been measured in situ (*i.e.*, under natural conditions, while still attached to surfaces) (Borole et al. 2011).

The role of biofilms in modulating the induced polarization response of biologically active subsurface systems was suggested by Davis et al. (2006), who measured increasing charge storage (σ'') during biofilm growth in biostimulated column experiments. Pore structure-induced changes, due to processes such as bioclogging, were postulated as the major drivers of biofilm-mediated SIP responses (Davis et al., 2006; Ntarlagiannis and Ferguson 2009; Davis et al. 2010; Wu et al. 2014). While bioclogging unequivocally mediates pore geometry, and therefore affects current flow and polarization, electromigration and charge storage within the biofilm matrix as well as within the bacterial surfaces concurrently contribute to the measured SIP responses (Abdel Aal et al. 2010). Albrecht et al. (2011) measured a strong correlation between phase shift (as large as 50 mrad, at 4 Hz) and biofilm volume growth in *Burkholderia sp.* (NAH1)-mediated phenanthrene degradation experiments. Identical experiments performed with a non-biofilm producing strain - *Stenotrophomonas maltophilia* (MATE10) showed similar growth kinetics, but 10 times lower phase shift magnitude. Rosier et al. (2019) measured increasing σ'' signals (characteristic peak-frequency between 1 and 10 Hz) with increasing cell density of *Pseudomonas aeruginosa* suspensions in experimental columns. The authors reported a direct dependence of measured SIP signals in response to artificially added biofilm components (alginate, phenazine and DNA), both from signal contributions of elevated concentrations of the components themselves, and when added to *P. aeruginosa* suspensions. Furthermore, they suggest that SIP can be developed to assess specific biofilm developmental changes.

Variations in biofilm constituents are a function of community development and microbial metabolic state and function. For example, the accumulation of phenazines can enhance extracellular electron

transfer, potentially yielding byproducts that affect polarization (Wang et al. 2014). Biofilm development requires extracellular DNA (eDNA), which can be produced by certain types of bacteria (Whitchurch et al. 2002). Cell lysis can also result in the release of large quantities of eDNA, which could suppress polarization, for example by eDNA-cation chelation (Mulcahy et al. 2008). The suppression of polarization (decrease in σ'') during cell lysis was previously reported by Davis et al. (2006). The complex nature of biofilm-mediated polarization mechanisms is clearly a function of the transient nature of biofilm development and the changes experienced or induced by the microbial community.

While efforts have already been made to isolate SIP signal contributions stemming from various biofilm components (*e.g.* Rosier et al. 2019), the determination of the sensitivity of SIP to specific biofilm development changes requires an experimental shift from suspension measurements to experiments under growth conditions. Time-lapse monitoring of both changes in biofilm composition and structure and concurrent SIP signals would allow us to develop direct linkages between a process of interest and variations to SIP-derived parameters (*e.g.* σ'', τ, M_n).

Extracellular electron transfer (EET)

The vast majority of bacteria take up soluble electron acceptors and donors. Some bacteria, however, have shown the ability to remotely access electrons either within adjacent solid (mineral) electron donors or at a distance (*e.g. Geobacter* spp. and *Shewanella* spp.) (Babauta et al. 2012; Nealson 2017). These electrochemically active microorganisms perform extracellular electron transfer (EET). They can form electroactive biofilms that have been extensively studied for the past two decades for their ability to generate electrical energy from biochemical energy in microbial fuel cells (Logan and Regan 2006). Both direct and indirect mechanisms have been proposed to explain the electron transfer from the cell-membrane of the bacteria located inside biofilms (sometimes more than 20-cell lengths away) to an external solid surface (summarized in Figure 3). The exact mechanisms, however, remain intensively debated (Borole et al. 2011; Babauta et al. 2012; Bond et al. 2012; Dominguez-Benetton et al. 2012; Beyenal and Babauta 2015). Due to the inherent sensitivity of induced polarization signals to

317 electrochemical processes within biofilms, and at the cell membrane-fluid interface, IP can be applied
318 to shed light on the mechanisms aiding EET.

319 ***Direct detection of microbial cells and biofilms using IP***

320 Geomicrobiological quantification techniques are destructive, and sample preparation often alters the
321 microbial metabolic state, when subjecting samples to detection-enhancing treatments (Vives-Rego et
322 al. 2000; Wardman et al. 2014). Furthermore, extracting in situ information of microbially mediated
323 reactions, at both the field and laboratory scales, requires destructive sampling methods and provides
324 only spatially and temporally scattered sampling points (*e.g.* Anneser et al. 2008; Mellage et al. 2015).
325 High spatiotemporal resolution IP measurements can fill the methodological gap highlighted within the
326 geomicrobiological literature (e.g. Kappler et al. 2005; Wardman et al. 2014) and provide non-
327 destructive information that is able to capture the adaptability of microbial communities at the field and
328 laboratory scales. The challenge in the adoption of SIP as a geomicrobiological measurement tool lies
329 in the inherent ambiguity of signal interpretation, due to the contribution of multiple properties and
330 processes. Thus, a better mechanistic understanding of the polarization processes involved not only by
331 the presence of the microbial cells themselves, but also by their interactions with their environment is
332 necessary. To solve this ambiguity, time-lapse IP measurements can also be part of the solution. They
333 record dynamic processes that change more rapidly than most petrophysical soil properties, effectively
334 normalizing the effect of the background signal contributions.

335 We envision that the production of further IP datasets, monitoring microbial dynamics, will help
336 calibrate IP tools directly applicable in biogeochemistry and geomicrobiology experimental setups. For
337 a specific porous medium, SIP signal changes can be used to directly compute microbial growth rates,
338 and, subsequently, rates of substrate turnover, simply by integrating electrode arrays into conventional
339 flow-through column and/or tank experiments. The availability of real-time data can aid in experimental
340 design, specifically when timing invasive sampling events. Conceivably, technological and theoretical
341 advances will eventually lead to similar quantitative applications at the lysimeter and field scales.
342 Improving our understanding of microbially mediated IP responses, laying the foundations for a unified
343 theoretical framework for polarization of bacteria and biofilms in porous media and developing IP tools

directly integrated in biogeochemical or geomicrobilogical experimental setups can help position IP as a bridge between our understanding of microbial dynamics, and our ability to measure it.

Microbially mediated processes and applications

Before detecting the polarization signature of subsurface microorganisms themselves, the first biogeophysical studies recognized the role of microbially mediated processes in the measured IP signal. Indeed, early observations showed 'anomalous' conductive signals at hydrocarbon contaminated sites (e.g. Bermejo et al., 1997; Atekwana et al., 2000; 2004a; 2004b), that were attributed to microbially-driven hydrocarbon degradation and the associated release of metabolic byproducts (Atekwana and Slater 2009; Atekwana and Atekwana 2010 and references therein). Most of the current biogeophysical work regarding microbial activity in the subsurface is still focused on microbially mediated processes. The main reasons for this are twofold: (i) there is an urgent need for characterization and monitoring of microbially mediated processes in contaminated environments, and (ii) the geophysical signals generated by the byproducts of microbial processes are significantly larger that the signal from the microbial presence or activity *per se*. Indeed, microbially mediated processes trigger physical changes (e.g. mineral precipitation, bioclogging at the grains surface, change in grain roughness) and chemical changes (e.g. mineral etching, mineral dissolution, redox reactions catalyzed by micro-organisms) that directly impact the resulting IP signal (Figure 4) (e.g. Atekwana and Slater, 2009; Heenan et al., 2013; Kimak et al., 2019). Common applications of the IP method in biogeophysics linked with microbially mediated processes include hydrocarbon spill characterization and monitoring (e.g. Flores-Orozco et al. 2012; Cassiani et al. 2014; Heenan et al. 2015; Ntarlagiannis et al. 2016, 2018; Kimak et al. 2019), contaminant sequestration and/or immobilization and mineral precipitation. In the last decade, new areas have also emerged, such as calcite biomineralization or OM characterization in peatland studies. In this section, we will present recent insights related to these applications before discussing direct detection of microbially mediated processes using IP.

Hydrocarbon degradation

Hydrocarbon impacted porous media appear to have a complex, but clearly measurable, IP signature that provides information on the hydrocarbon contaminant and on the biogeochemical processes associated with the hydrocarbon degradation (Davis et al. 2006; Schmutz et al. 2010, 2012; Ustra et al. 2012; Heenan et al. 2013; Personna et al. 2013b; Kessouri et al. 2016; Fernandez et al. 2018; Kimak et al. 2019). One of the main reasons for the complex behavior of the signature lies with the nature and the properties of hydrocarbons. Non-polar (i.e., non-wetting) hydrocarbons tend to increase the IP signature of the subsurface (Revil et al. 2011; Flores-Orozco et al. 2015; Johansson et al. 2015), while polar (i.e., wetting) ones have shown to either increase (Vanhala 1997; Kemna et al. 2004; Deceuster and Kaufmann 2012) or dampen the IP effect (Ustra et al. 2012; Personna et al. 2013b). In addition, environmental conditions (e.g. geology) and biodegradation of hydrocarbons through redox reactions, leads to additional physical and chemical changes in the subsurface with measurable IP signatures (Figure 4), which introduces ambiguity in data interpretation (Personna et al. 2013a ; Ntarlagiannis et al. 2016, 2018; Fernandez et al. 2018; Kimak et al. 2019).

IP applications at the field scale are becoming increasingly common (Deceuster and Kaufmann 2012; Flores-Orozco et al. 2012, 2018; Ntarlagiannis et al. 2016, 2018), yet the interpretation of imaging results is still open to debate. Studies have shown that the IP response tends to increase with subsurface hydrocarbon concentration (Flores-Orozco et al. 2015; Johansson et al. 2015) and this is often attributed to microbially mediated degradation of hydrocarbons. On the contrary, there are observations with negligible polarization in the case of oversaturation of hydrocarbons and/or the presence free-phase non-aqueous phase liquids (NAPL) (Flores-Orozco et al. 2012). Complex subsurface conditions, including infrastructure and groundwater level changes, can also contribute to non-trivial IP interpretation (Flores-Orozco et al. 2018).

Laboratory research is paving the way for quantitative interpretation of IP signals for hydrocarbon biodegradation. The links of IP signals to the type of hydrocarbon (e.g. Schmutz et al. 2010; Revil et al. 2011; Ustra et al. 2012; Personna et al. 2013b) and to bioremediation processes (e.g. Heenan et al. 2013; Kimak et al. 2019) have been identified. The next step should be to quantify these signals and try to deconvolute the spectral response of remediation processes in complex environments.

Advances are also being made in modeling. For example, Bücker et al. (2017) proposed an extension of the analytical model for membrane polarization to study the IP effect associated with the presence of both "wetting" or "non-wetting" hydrocarbon compounds in the pore space. Their model is consistent with field and laboratory observations, describing a decrease of the IP response with hydrocarbon saturation in the case of wetting hydrocarbons and in high saturation cases for non-wetting ones. Depending on the surface properties of the particular hydrocarbon contaminant, the extended model (Bücker et al. 2017) also explains increased IP responses at intermediate hydrocarbon concentrations. Biodegradation of hydrocarbon, as well as stimulated microbial activity, still need to be taken into account in the modelling of the polarization mechanisms.

Mineral precipitation

In subsurface remediation strategies, typically, the desired result is complete removal or degradation of the contaminant. For some forms of contaminants that cannot be degraded (e.g. radionuclides and toxic metals), alternative remediation approaches can consist in immobilization or sequestration in situ. A common example is urea hydrolysis based co-precipitation of radionuclides with calcite, as shown in Figure 5 (Colwell et al. 2005; Fujita et al. 2008, 2010; Wu et al. 2011; Smith et al. 2012). Urea hydrolysis is catalyzed by the urease enzyme, expressed by many microorganisms in the subsurface to harvest nitrogen.

Monitoring tools are needed to assess the efficiency of immobilization or sequestration remediation approaches. IP has been suggested, and tested, as a complementary method. Contaminant immobilization in mineral phases often leads to changes in pore chemistry and fluid-mineral interfacial charge properties. Given its sensitivity to capture changes in these parameters, the IP method has great potential for monitoring contaminant immobilization in mineral phases.

Another potential application of the IP method is in soil enhancement projects. A common approach to increase soil strength/stiffness is through the precipitation of a new mineral phase such as calcite. Microbially induced calcite precipitation (MICP) is taking advantage of the same ureolytic processes (Figure 5) but with a different objective. MICP generally results in biomineralization of calcium

carbonate, where the dominant stable mineral phase is calcite (Saneiyan et al. 2019). Calcite acts as a binding agent in the soil and could be used for crack remediation, erosion prevention, dust control and infrastructure engineering applications (e.g. supporting foundations, restoration of limestone buildings) (DeJong et al. 2010; DeJong et al. 2013; Dhami et al. 2013).

Monitoring studies including SIP measurements successfully established the method's sensitivity to calcite precipitation and provided quantitative information on the precipitation rates (Wu et al. 2008, 2009, 2010, 2011; Saneiyan et al. 2018). Experiments on abiotic calcite precipitation on glass beads at the bench-scale show that SIP responses to calcite precipitation exhibit peak frequencies between 100 Hz to 1 kHz (Wu et al. 2010). Ottawa sand and sand-clay mixtures show SIP peak relaxation frequencies between 1 mHz to 1 Hz (depending on soil mixture type) (Saneiyan et al. 2018). MICP processes had similar SIP signatures; however, with higher signal magnitude (higher maximum phase amplitude). This difference can be due to different precipitation patterns and processes, the impact of microbes and/or mineral distribution style (Saneiyan et al. 2016). A recent field study from Saneiyan et al. (2019) demonstrated the benefit of IP monitoring during a field application of MICP, where IP succesfully provided near real time information on MICP progress. Further research is needed to extract quantitative information on calcite precipitation rate from field TDIP measurements.

Another benefit of MICP is the potential for atmospheric CO_2 sequestration, as well as Ca^{2+} removal from wastewater, rendering the IP method a potential monitoring tool for engineering solutions to climate change (Hammes et al. 2003; Wanjari et al. 2011; Yadav et al. 2011).

Organic matter and peatlands

A very promising application of the IP method is the study of soil organic matter (SOM). The creation and decomposition of SOM, catalyzed by micro-organisms, is a key factor in the carbon cycle, and subsequent greenhouse gas emissions and retention of nutrients and contaminants (Lehmann and Kleber 2015). Monitoring SOM properties and stocks is therefore of great importance, but also highly challenging due to the complex interactions between SOM and soil minerals, spatial heterogeneity, and SOM dynamics. These challenges call for geophysical methods, from which the IP is the best candidate

449 due to its high sensitivity to cation exchange capacity (CEC), a characteristic SOM property (Vinegar
450 and Waxman 1984).

451 Early studies were successful in linking IP with organic soil depth (Slater et al. 2002), and the
452 decomposition state of peat (Kettridge et al. 2008) in peatlands. Schwartz et al. (2014) examined the
453 impact of SOM on the IP signature of soil, and successfully linked the IP signals with the SOM, soil
454 mineral interactions, and the chemical composition of the soil solution. Furthermore, Walter et al.
455 (2015) reported a strong correlation between peat CEC and quadrature conductivity (IP parameter),
456 while Ponziani et al. (2012) could not find any correlation between the IP response and various sample
457 characteristics such as decomposition state, water content, organic content and CEC.

458 The above studies demonstrate both the great potential of the IP method to characterize and monitor
459 SOM and peatlands, but also the need for more studies that will clarify the governing mechanisms
460 controlling the IP signature of SOM and its dependence on biogeochemical properties and processes.

461 ***Direct detection of microbially mediated processes using IP***

462 As an indirect method, interpretation of IP signals is always challenged with non-uniqueness and
463 ambiguity. For example, in the case of contaminant immobilization/sequestration monitoring, it is very
464 challenging to directly link IP signals with the rate or concentration of metal sequestrated in the host
465 material. The same applies to hydrocarbon degradation studies: IP can be used to monitor degradation,
466 and even biogeochemical activity, but exact interpretation of the stage of the hydrocarbon or the
467 concentration is far from trivial. While numerous laboratory-based studies have established the
468 sensitivity of IP signals to a variety of targets (e.g. precipitation processes that are potentially effective
469 at immobilizing or sequestering contaminants, hydrocarbon contaminants), application of such
470 monitoring approaches in the field has been sparse. This is largely attributed to the inter-twined and
471 interactive processes, such as changes in lithology, soil structure, and moisture dynamics, each having
472 its own IP characteristics that complicate the decoupling of those signals associated with the
473 contaminant sequestering precipitation processes. To solve this challenge, future studies need to couple
474 IP measurements with direct biogeochemical measurements and mechanistic models. Further research
475 effort will need to be spent on the development of such mechanistic models for better understanding

476 the IP signal, as well as making links with underlying reaction mechanisms. As demonstrated in Wu et
477 al. (2011), while geophysical approaches provide indicator signals of system dynamics, mechanistic
478 models, such as reactive transport modeling are important to help understand changes that drive
479 geophysical signatures.
480

481 # Root characterization

482 An emerging area of research in the near-surface geophysics community is the use of IP measurements
483 to investigate plant root systems. Root system architecture plays an important role for plant water
484 uptake, and thus affects both the hydrological cycle and the land-surface energy balance. In addition,
485 root water uptake is directly related to crop growth, playing an important role in agricultural food
486 production. Geophysical methods, and particularly IP, need to be evaluated as non-destructive methods
487 to characterize and monitor plant root systems. Vanderborght et al. (2013) extensively reviewed the use
488 of electromagnetic methods sensitive to conduction and polarization processes for root investigations:
489 ground penetrating radar (GPR), electrical resistivity tomography (ERT), and IP. The magnitude of the
490 complex electrical conductivity, through ERT, has been extensively used to image soil water content
491 changes associated with root water uptake (e.g. Garré et al. 2011; Cassiani et al. 2015). In the following
492 subsections, we first describe the known electrical behavior of a root, before reviewing studies
493 characterizing the IP signal of single roots and plant root systems. We then review imaging studies of
494 plant root systems in their environment (soil or hydroponic solution) using indirect current injection
495 methods. We finally develop a conceptual model that summarizes our current understanding of the IP
496 signature of root cells.

497 ***The root structure and its electrical behavior***

498 A key issue with the use of ERT for the direct detection of roots is that the expected contrast in electrical
499 properties between soil and roots is ambiguous in the presence of soil water content variation, since the
500 real part of the conductivity of plant roots is expected to fall between the values for dry and saturated
501 soil. The contrast in the imaginary part of the electrical conductivity between soil and roots is expected
502 to be stronger because of electrical polarization processes associated with the EDLs that exist at charged

503 interfaces associated with roots. In particular, the inside of the roots consists of cells that are known to
504 have a plasma membrane and an associated EDL (e.g. Wang et al. 2011) that is expected to polarize.
505 The outside of the root consists of an epidermis surrounding a cortex, both composed of cells and
506 expected to provide a resistive barrier to current flow.

507 ***IP signature of single roots and root system***

508 An example of the frequency-dependent electrical properties of a single root segment is shown in Figure
509 6. It can be seen that the magnitude of the resistivity varies between 3 and 10 ohm.m for an 8-day old
510 maize root. At the same time, the measured phase increases strongly with frequency up to a maximum
511 of 400 mrad at 10 kHz. This high relaxation frequency suggests a relatively small length-scale of
512 polarization. The electrical properties of root segments cannot be obtained using in situ measurements.
513 Therefore, several studies have used so-called stem-based excitation methods to investigate the
514 electrical properties of root systems. In this approach, the electrical properties of roots are determined
515 by measuring the electrical potential that results from the application of an electrical field between two
516 electrodes, one of them in the plant stem, and the other one in the growing medium (soil or hydroponic
517 solution). Given the relatively low resistivity of segments of young roots (see Figure 6), it may be
518 expected that current flows preferentially through the roots in this type of set-up. Chloupek (1972) was
519 one of the first to apply this method and reported a correlation between root mass and root electrical
520 capacitance at 1 kHz (the electrical capacitance, the imaginary part and the phase of the electrical
521 conductivity are all related to energy storage processes). Since then, a linear relationship between root
522 mass and root electrical capacitance has been reported by several authors (Kendall et al. 1982; van
523 Beem et al. 1998). Given the strong polarizability of root segments shown in Figure 6, these
524 relationships are not surprising. These results are usually interpreted using the electrical circuit model
525 proposed by Dalton (1995). In this model, the root behaves like a cylindrical capacitor and the root
526 system capacitance can be obtained by summing (in parallel) the capacitance of each root segment. A
527 different circuit model was proposed by Dietrich et al. (2012), who suggested that the root behaves like
528 a continuous dielectric material embedded in a medium of higher capacitance. The theoretical

consequence of this alternative model is that the capacitance measured between the root and the soil/hydroponic medium is related to the root cross-sectional area (Dietrich et al. 2012, 2013).

In several studies, multi-frequency measurements of the electrical properties of root systems were made. For example, Cao et al. (2011) made two-point SIP measurements in the Hz to kHz frequency range) to separate between the root and stem capacitances and achieved a better correlation between root traits and root electrical properties than in single frequency measurements. The importance of multi-frequency measurements was recently also emphasized by Postic and Doussan (2016), who showed that the correlation between root traits and electrical properties is frequency dependent. Again, this is also consistent with the strong frequency-dependent phase response of root segments shown in Figure 6.

Imaging of the IP response of root systems in their environment

Time-lapse IP imaging is required to spatially and temporally differentiate root structure and activity. So far, distinct polarization signatures of non-woody crop roots have been reconstructed from spectral IP 2D or 3D images in controlled laboratory experiments on root systems embedded in aqueous solutions (Weigand, 2017; Weigand and Kemna, 2017; 2019). These studies showed that the spatial resolution of IP imaging is not sufficient to resolve single roots, but that the root extent can potentially be reconstructed. Interestingly, the frequency dependence of the electrical properties of root signals was also evident in the imaging results (see Weigand and Kemna, 2017), providing potential to improve measurement results by careful selection of measurement frequencies. This will be especially helpful in cases where the electrical properties of both soil and root exhibit strong frequency dependence.

Apart from providing information on the root system extension, it has also been shown that spectral IP imaging can capture information on functional processes within the root system. For example, Weigand and Kemna (2017) showed a temporal and spatial decrease of polarization strength during prolonged nutrient deprivation of oilseed plants, indicating a sensitivity to nutrient uptake and translocation mechanisms. This is further supported by the observation that decapitated plants, which cannot take up water and nutrients, did not show a decrease in electrical polarization under nutrient deprivation (Weigand and Kemna 2019).

555 A remaining challenge is the direct imaging of root systems in soil. In such systems, interpretation is
556 complicated by the superposition of root signatures and soil polarization signatures and associated
557 processes, such as water dynamics, salinity and temperature changes (e.g. Mary et al. 2017; Weigand
558 2017). In particular, the SIP response of unsaturated soil is still poorly understood (e.g. Breede et al.
559 2012; Maineult et al. 2018). Early attempts to image coarse root systems under controlled field
560 conditions using simple mapping approaches showed promising results, but highlighted the importance
561 of incorporating anisotropy into the measurement and analysis procedures (Mary et al. 2017). Possible
562 solutions might also be found in the combination of imaging with stem-injection setups, as recently
563 done by Mary et al. (2018) for grapevine root systems using resistance measurements. The approach
564 combines both increased current flow (information content) through the root system with the spatial
565 differentiation of imaging methods. Finally, multi-frequency measurements also seem essential for root
566 investigations in soils and substrates. Such measurements not only help in differentiating between soil
567 and root system (Mary et al. 2017), but also allow to extract characteristic relaxation times from the
568 imaging results, which may provide information on the length scales of the polarization processes (e.g.
569 Weigand and Kemna 2019).

570 ***Conceptual model of IP response of plant root systems***

571 In order to make progress in the study of roots with IP measurements, a "phyto-physical" model that
572 connects root electrical signatures to root properties will need to be developed. On the one hand, this
573 will require a deeper experimental understanding of energy storage processes within roots (measured
574 as electrical capacity or polarization) and their relation to root anatomy and physiology. This can best
575 be achieved with dedicated laboratory experiments that aim to link the frequency dependent electrical
576 properties of roots to root properties (root diameter, surface area, biomass, etc.) and root activity (ion
577 transport, membrane potential, etc.). On the other hand, there is a clear need to support the experimental
578 work with a theoretical framework that goes beyond the currently used electrical circuit models and
579 links electrophysiological models of cells to electrochemical models that simulate electrical polarization
580 (e.g. Bücker and Hördt 2013).

581 Recently, Weigand and Kemna (2019) proposed a first step towards such a theoretical framework in
582 order to explain diurnal variations in IP response associated with variations in nutrient uptake. They
583 proposed a conceptual electrochemical model at the root cell scale that is detailed for the first time
584 below and illustrated in Figure 7. It integrates established relationships between cell membrane
585 electrical characteristics and cross-membrane ion transport (Kinraide 2001; Wang et al. 2011) with the
586 mechanistic understanding of electrochemical polarization around charged, electrically conductive
587 particles (Wong 1979; Bücker et al. 2018, 2019). In particular, Kinraide (2001) proposed a model to
588 describe the ion flux across the cell membrane as a function of the ion activities and electric potentials
589 at the inner and outer surfaces of the membrane. In this model, a Gouy-Chapman-Stern model of the
590 electrical double layer is used to describe the electrical potentials at inner and outer surface of the
591 membrane. Changes in the typically negative surface electric potential on the outside of the membrane
592 (φ_0 in Figure 7) are offset by changes in the transmembrane potential difference that controls the gating
593 of ion channels and ion fluxes across the membrane ($\Delta\varphi_{PM}$ in Figure 7). Thus, a decreased negativity
594 of φ_0 corresponds with an increased cation flux (j_{up} in Figure 7) (and decreased anion flux) into the
595 cell, and vice versa (see Figure 7) (Kinraide 2001; Wang et al. 2011). A decreased negativity of φ_0,
596 which is directly related to the surface charge density of the membrane (Kinraide and Wang 2010),
597 results in a weaker EDL at the outer membrane surface and thus a decreased polarizability of the EDL
598 in an external electric field (Figure 7). As such, the proposed polarization mechanism is similar to the
599 electrochemical polarization around metallic particles, where charge transfer reactions at the
600 electrolyte-metal interface cause a weakening of the EDL and consequently a reduced polarizability
601 (Wong 1979; Bücker et al. 2018, 2019).
602 This conceptual model implies an inverse relationship between the magnitude of the IP response of root
603 systems and the strength of cation uptake and is able to qualitatively explain the diurnal variations of
604 the IP magnitude recently observed by Weigand and Kemna (2019). However, it is still unclear how
605 the model can be appropriately scaled up to an entire root system. Also, it is yet unclear whether the
606 internal structure of roots may give rise to effective polarization at scales larger than the cell scale. The
607 analysis of the spectral IP imaging results of various experiments by Weigand and Kemna (2019)

608 yielded relaxation time estimates in the microsecond range, suggesting length scales of the underlying
609 polarization processes of several micrometers (Weigand and Kemna 2019). This is in agreement with
610 the proposed cell-based conceptual model, but the experimental basis is not broad enough to draw
611 definite conclusions yet.

612 ***Research directions and applications***

613 Based on the first studies on plant root systems, the IP method represents an interesting tool to map the
614 root distribution and monitor soil-root interactions. Indeed, the IP method could complement or even
615 partly substitute rhizotube or trenching methods. Given that those established methods also have large
616 associated uncertainties (due to being either point measurements, or manually counted/drawn), IP
617 uncertainties linked with the stacking of multiple polarization mechanisms might not be too disruptive.

618 In addition, time-lapse IP measurements could be used as an affordable environmental monitoring tool,
619 and, e.g., indicate when the physiological equilibrium of a plant-root system is reached. This envisioned
620 application is based on a qualitative analysis of the IP data, and thus could be used, even when a full
621 understanding of the underlying (polarization) mechanisms associated to roots is lacking.

622 In the near future, IP may also be used to support the conceptualization and calibration of physiological
623 models, such as root water uptake models, which can then be easily connected to various kinds of local
624 to global modeling/forecasting frameworks. The observed sensitivity of the IP signal to nutrient uptake
625 is particularly exciting, since it suggests a potential to separate root structure and function using non-
626 invasive measurement.

627

628 ## Wood and tree characterization

629 Besides the description of microbial processes and root systems, IP can also be used to characterize
630 wood and tree structures. The electrical properties of wood have been studied for almost a century.
631 Indeed, Stamm (1930) used an electrical instrument to determine the moisture content of wood. Shigo
632 and Shigo (1974) developed an electrical instrument to detect discoloration and decay in living trees
633 and creosoted utility poles. In the following years, further instrumental development allowed increasing

634 the range of applications such as tree root detection (e.g. Piirto and Wilcox, 1978; Zürcher, 1988; Brandt
635 and Rinn, 1989). Later, electrical measurements in tree trunks showed that tomographic examinations
636 are suitable for reproducing the internal structure of a living tree, for observing possible fluid transfer,
637 for detecting decay and infections or for separating different wood sections (e.g. Weihs et al 1999,
638 Nicolotti et al. 2003; Al Hagrey 2006; Bieker and Rust 2010; Bieker et al. 2010; Guyot et al. 2013).
639 Schleifer et al. (2002) showed that wood is a polarizable material and were able to detect historically
640 important wood structures in the subsurface using the IP method. In addition to information extracted
641 from electrical resistivity, the phase shift is sensitive to additional wood parameters such as wood cell
642 structure, and can thus be used for various applications such as the assessment of fungal infection and
643 thus tree stability (Martin 2012; Martin and Günther 2013) or the classification of different tree species
644 (Martin et al. 2015). Furthermore, phase shift evaluation has the potential to detect the maturation status
645 of trees and therefore estimate the best time for tree felling (Martin et al. 2015).

646 ***Factors affecting the IP signal of tree wood***

647 The interpretation of the IP signature in wood and trees is very much affected by the heterogeneity and
648 the strong anisotropy of wooden material. Martin (2012) measured the laboratory IP signature of healthy
649 oak wood samples and observed that both resistivity and phase shift of the wood samples vary with
650 their position within the tree. The lowest resistivities with the highest phase effects are measured for
651 samples extracted from regions where all the fluid transport in the tree trunk occurs.

652 Besides anisotropy, different tree species also influence the IP signals due to their different wood
653 structure. For example, Martin et al. (2015) showed that the polarization of different European tree
654 species (e.g. beech, oak, lime) differ significantly both in terms of chargeability and peak frequency.
655 Tropical wood can be separated and classified from other wood (e.g. European) due to an often-higher
656 polarization effect (up to 140 mrad) and a peak frequency at very low frequencies (< 0.01 Hz). In
657 particular, sandalwood trees can be monitored using IP (Martin et al. 2015). These trees react to injuries
658 by producing oil and oil-bearing ingredients within the tree, which affect the IP response: the phase
659 shift increases significantly with oil content. The IP method can thus be used to determine the best time
660 to cut down the tree and collect the highest (very valuable) oil concentration (Martin et al. 2015).

Additionally, fungal infection of trees has a measurable impact on the IP signature. Martin (2012) showed that fungal infections destroy polarizable wood cells in the laboratory. With increasing fungal infection, the IP phase signal decreases continuously, whereas the resistivity mainly reflects the wood moisture and dissolved ions. These laboratory findings were verified by tomographic (2D) field applications on tree trunks at different heights (Martin and Günther 2013). The infected parts of an oak tree wood showed a decrease in resistivity (due to the moisture of the fungi) and decrease in phase.

At the field scale, the IP signal is not only sensitive to the presence of fungi but will also vary with the environment. Indeed, a living tree is affected by the seasons, the weather and the tree location. In contrast to "dead" wood used for laboratory measurements, the influence of the environment must also be considered for field data interpretation of living trees (Figure 8). For example, the tree stops the water and nutrient transport in autumn and winter, which affects the electrical properties

Research directions

In the last 10 years, many successful and promising experiments have shown that the IP method is sensitive to changes in wood and tree structures. However, for a deeper understanding of the polarization processes and before any commercial application, further research is still needed. Future laboratory experiments should be geared towards understanding the effects of different kinds of fungi under varying environmental conditions and tree species. Tomographic field investigation for different tree species are also required to explain the IP signature of different tree species. In addition to the applications mentioned herein, experiments could be made in the laboratory and the field to test IP's sensitivity to estimate the hydraulic conductivity in wood or trees and to separate the influence of water salinity. The field measurement setups also need to be adapted (e.g. electrode material, configuration, instruments, etc.) for IP measurement on wood. Finally, a better understanding of the physiological processes involved in the polarization mechanisms must be achieved to be able to better interpret the IP signals collected from this living material. This requires further efforts for developing mechanistic models linking the tree physiological responses to their IP signatures.

The IP method can provide additional information, such as the localization of hidden wooden structures (e.g. Schleifer et al. 2002), the condition of wood or the stability status of the tree (e.g. Martin et al.

688 2012, 2013) that are hard to evaluate non-destructively with other methods. Many additional
689 applications of the IP method for tree and wood can thus be envisioned. IP measurements can be
690 particularly interesting for archaeological and forestry applications, as well as for stability studies of
691 road trees and wood poles and/or to understand tree physiology in agricultural and ecological studies
692 (see Figure 8).

693 ## From the laboratory to the field scale

694 In the previous sections, it was clearly shown that IP signals are sensitive to biological changes and
695 processes, both at the microscopic and macroscopic scales. The IP method can indeed be used at various
696 scales, measuring the same parameters, but scaling (up or down) the observations is a non-trivial issue
697 that needs further research efforts. In this section, we summarize the state-of-the-art up- and down-
698 scaling methods, the current challenges and point out at future research directions.
699
700 At the laboratory scale, it is possible to conduct experiments in a controlled environment, and to
701 consider macroscopically homogeneous samples to individually investigate the different parameters
702 and processes that affect the IP response. In addition, complementary analyses can be used to better
703 understand the associated biogeochemical mechanisms. The combination of IP measurements and
704 complementary physical, chemical and biological analyses can even lead to the development of
705 petrophysical relationships that can be used by biogeochemists or plant/crop scientists as a proxy to
706 monitor their experiments at various scales due to the multi-scale adaptability of the IP method.
707 Laboratory investigations are also strongly needed to interpret field scale experiments. Thus far, the
708 transferability of laboratory observations to field applications is challenging due to: (i) the change in
709 the investigated representative volume; (ii) the higher complexity of the system in the field in terms of
710 heterogeneity of soil properties (water content, soil composition, salinity, pH, temperature) and
711 interactions between different processes; (iii) the change in measuring equipment, methodology and
712 measurement sensitivity.
713

714 At the field scale, IP measurements are affected by a variety of influences such as soil properties, water
715 chemistry or environmental changes, resulting in a superposition of different IP signals. For example,
716 Weigand (2017) showed that the IP response from non-woody crop roots are hard to measure due to the
717 small resistivity contrast with the surrounding subsoil and the small volume of root biomass. Changes
718 in the environment can not only mask the microbial, root or tree signatures, but also change them as
719 they react to their environment. Weigand and Kemna (2019) observed changes in the chargeability of
720 the roots that reacted physiologically to varying sunlight. The interpretation of field IP signals thus
721 requires an understanding of the biogeochemical dynamics.
722 Furthermore, some biological processes that are observed in the laboratory show IP signatures at very
723 low frequencies, which are hard to measure in the field due to the large amount of time such field
724 surveys would take, compared to the reaction time scale of the monitored biological phenomena. For
725 instance, Martin and Günther (2013) could differentiate fungal infected wood and healthy wood through
726 their phase variations only below 0.1 Hz. However, full-scale tomography on actual tree trunks was not
727 possible with commercially available equipment at such low frequency because of time constraints.
728 High spatio-temporal resolution and information at a broad frequency-range in the field is also
729 important for the characterization of geochemical processes accompanying microbial activity using SIP.
730 For example, extensive monitoring investigations at the Rifle study area (Colorado, USA) were
731 performed to assess the stimulation of iron-reducing bacteria for the immobilization of uranium in
732 groundwater. Initial campaigns performed at a single frequency (1 Hz) demonstrated the applicability
733 of the IP method to assess the precipitation of iron sulphides (Williams et al. 2009).The extension to a
734 broader frequency range (0.06 to 10 Hz) demonstrated the possibility to also gain information about
735 changes in subsurface redox-status (Flores-Orozco et al. 2011). An even broader frequency range (0.06
736 to 256 Hz) allowed Flores-Orozco et al. (2013) to determine a characteristic relaxation frequency that
737 provided information regarding the dominant grain size controlling the polarization mechanism.
738 Although other studies have demonstrated the possibility to perform SIP measurements in a broad
739 frequency range (e.g. Flores-Orozco et al. 2012; 2018; Gallistl et al. 2018), applications are still rare
740 due to the extensive acquisition times (for measurements at frequencies below 1 Hz), and the
741 contamination of the data due to parasitic electromagnetic effects (specially at frequencies above

742 50 Hz). This can be improved by adapting existing field measurement setups and by developing further
743 FDIP field measurement equipment (e.g. Dahlin and Zhou 2006; Flores-Orozco et al. 2013; Kelter et
744 al. 2018). Correction methods for capacitive and inductive coupling effects have also been developed
745 for borehole (Zhao et al. 2013, 2015), and surface FDIP measurements (Zimmermann et al., 2019), but
746 have not yet been transferred to commercially available measurement equipment.
747 Another issue for upscaling laboratory results to field applications is that the IP methodology in
748 laboratory and field measurements are not always practically equivalent. TDIP and FDIP measurements
749 may provide different resolution and spectral ranges due to instrumentation and configuration. In
750 laboratory experiments, where time constraints are smaller, mostly SIP measurements are used due to
751 their better spectral resolution and signal-to-noise ratio. To obtain the same high-quality wide-range
752 data as in the laboratory, more effort and time are required for field measurements in the case of SIP
753 measurements compared to TDIP measurements. Therefore, in the field, TDIP measurements may be
754 more convenient and timesaving when using multi-core shielded cables and considering short
755 acquisition times (Olsson 2018). However, spectral information is lost using TDIP, especially at early
756 (high frequencies) and late times (lowest frequencies). To improve TDIP field data quality, full
757 waveform acquisition is a powerful tool that will help bridging the gap between SIP laboratory
758 measurements and TDIP field acquisition. A second type of challenges with field applications is
759 associated with the difficulty of acquiring high-quality data as well as the reduced resolution at depth.
760 The IP signature of the targeted biogeochemical process is then often smeared by large lithological
761 contrasts. Using different instruments, electrode material, cables (shielded or not), etc. can also cause
762 different parasitic signals, noise levels, spectral range as well as resolution and must be considered when
763 trying to upscale laboratory results (Dahlin et al. 2002; Dahlin and Leroux 2012; Zarif et al. 2017). Due
764 to the significant but often small phase variations in the laboratory IP signature of biological material
765 (Ntarlagiannis et al. 2005), it is even more necessary to ensure suitable system performance and thus
766 good-enough measurement sensitivity to small biological signatures in the field.
767
768 Despite the incomplete understanding of IP signal sources and the different measurement techniques,
769 field measurements are very useful, especially to study temporal processes (see above-mentioned time-

770 lapse field monitoring studies by Flores-Orozco et al. (2013)) or biological processes in a living system
771 such as standing trees that cannot be transferred to the laboratory. Indeed, Martin and Günther (2013)
772 observed different biological behaviour in living trees compared to (dead) wood samples. Moreover,
773 significant progress has been made in recent years to compare laboratory and field scale IP results linked
774 with biogeochemical processes. For instance, Saneiyan et al. (2019) demonstrated at the field scale, that
775 the imaginary conductivity signal tracks subsurface MICP (microbial induced calcite precipitation)
776 changes more clearly than just resistivity, which was in good agreement with their laboratory
777 observations (Saneiyan et al. 2018).
778
779 To further improve our understanding and interpretation of biogeochemical processes at the laboratory
780 and field scale, deduced from IP signal changes, we propose the following bridging framework (see
781 Figure 9). Laboratory experiments need to be conducted to quantitatively separate the effects of
782 different biogeochemical processes and to build a modeling framework that can be used for direct
783 laboratory applications or upscaling to field observations. Field campaigns also need to be led on well-
784 characterized field sites (access to temporally and spatially dense biogeochemical information), using
785 a broad frequency range. They can then be used to assess the applicability and/or improve the modeling
786 framework. Finally, the development of experiments at an intermediate lysimeter scale can be the
787 answer to: (i) upscaling the modeling framework from laboratory observations to uncontrolled field
788 measurements and (ii) studying the effect of heterogeneities on the IP signal.
789

790 # Joint interpretation

791 Joint interpretation is the concurrent use of (i) different geophysical datasets or (ii) IP and non-
792 geophysical datasets to assess the biological, chemical and physical state of the subsurface. Joint
793 interpretation of different geophysical datasets will not be discussed here, as it is not specific to IP nor
794 to biogeophysics. Rather, we focus on the use of IP data to calibrate a mechanistic model that contains
795 the general understanding of a biogeochemical process. As biogeophysics is relatively new, there are
796 very few examples of such joint interpretation in the literature. Hence, this section is intended as a

discussion of potential directions, rather than a critical review. It must be said upfront that soil systems in general, and soil biogeochemical systems in particular, are inherently complex and characteristically generate many different dynamic signals, natural or induced. This makes the interpretation of biogeophysical signatures more challenging than conventional geophysical signatures. Even in a controlled laboratory environment, it is difficult to isolate a sub-system, and the interpretation almost always needs additional sources of data. Incorporation of additional data is often done in a process modeling framework (Figure 10).

Joint interpretation of biological processes

Recently, (bio)geochemically induced changes in IP responses have been coupled to reactive transport models (RTMs), a combination which has resulted in the improvement of IP data interpretation, model formulation and biogeochemical system understanding (Wu et al. 2011, 2014; Mellage et al. 2018a and 2018b). In abiotic experiments, Mellage et al. (2018a) developed a coupled SIP-sensing and transport simulation framework to fit the breakthrough behavior of iron-oxide nanoparticles in natural aquifer sand. This simulation framework yielded direct quantitative relationships between nanoparticle concentration in the porous medium and measured SIP responses. The nanoparticle concentrations could only be inferred from outflow samples, but could be directly computed within the experimental domain by an RTM. In biotic sand column incubation experiments, Mellage et al. (2018b) coupled a diffusion-reaction model to SIP measurements. The integration of geophysically-derived parameters (e.g. relaxation time) improved the process-based conceptual understanding of their experiments, in turn improving the numerical model calibration. In similar systems, IP data can be used to either replace conventional breakthrough data, or better, used jointly with breakthrough data to better understand a system. A joint approach is inherently superior for non-conservative transport, where data regarding accumulation typically are only available at the end of a conventional breakthrough experiment. The integration of RTMs with SIP datasets therefore provides a framework for upscaling the approach to the field, where large-scale modelling approaches could benefit from more spatially and temporally comprehensive datasets. The challenge lies in the integration of methods, such as SIP, with existing modeling frameworks. Biogeophysical data do not relate directly to RTM-generated outputs (e.g.

824 geochemical speciation data, reaction rates and solute concentrations).Therefore, the establishment of
825 relationships between model parameters and method-specific outputs (i.e., conductivity) is required (Li
826 et al., 2017). The development of an integration framework would require bench-scale experiments to
827 develop the relationships between the techniques applied and the targeted information we are trying to
828 gather. For example, high resolution biogeophysical signal changes can be related to specific processes
829 via computed reaction rates. This would allow for the development of system-specific semi-quantitative
830 relationships that can be applied to inform and setup a larger-scale model at an analog field site (Figure
831 10).

832 ***Joint interpretation of biological activity byproducts***

833 While many challenges exist for direct coupling between SIP signals and RTMs, perhaps a more
834 developed application of IP is its utilization to monitor by- and end-products of reactive transport
835 processes. Such products include (i) emergence or disappearance of minerals, (ii) changes in pH or ionic
836 strength and speciation, or (iii) changes of the physical structure of the system (e.g. permeability) due
837 to dissolution or deformation. Among these studies, the application of IP to monitor mineral
838 precipitation during biogeochemical processes has been a major topic of interest. For example, studies
839 conducted by Williams et al. (2005) and Ntarlagiannis et al. (2005) investigated the SIP signals
840 associated with microbially induced sulfide precipitation and Wu et al. (2010) studied the SIP signature
841 of calcite precipitation. In relevant studies, Personna et al. (2008), Zhang et al. (2012), Hubbard et al.
842 (2004), and Placencia-Gómez et al. (2013) studied processes relevant to mineral surface dynamics,
843 including mineral transformation, surface absorption/desorption, as well as mineral transformation
844 during redox reactions. While such studies have collectively demonstrated the sensitivity of SIP signals
845 to the by-products of biogeochemical processes, the way SIP signals can be better related to reactive
846 processes in the mineral-water system is still poorly explored. Wu et al. (2011) developed a joint
847 interpretation concept, relating between SIP signals that originate with calcite deposition, and a reactive
848 transport model. Yet this is only a conceptual approach that needs further improvements in the context
849 of calcite and also requires generalization.

850 ***Remaining challenges***

The potential of SIP signals to help understand fundamental biogeochemical processes has been adequately demonstrated in the laboratory. However, IP datasets are difficult to self-interpret as they result from the addition of different IP signatures (e.g. the soil-water system, the biological components, and interaction with the soil system). A modeling framework that looks at the mechanics of the studied process (remediation, precipitation, etc.) and is calibrated using both IP and non-geophysical data, is a promising way to integrate such datasets at various scales from laboratory to field studies (Figure 10).

Because the geophysical field and the biogeochemical field communities are not traditionally overlapping, communication and interactions are critical to better understand the strength and needs of each community and facilitate the joint development of biogeophysics. For example, whether IP signals contain rates and speciation information that can help to better validate biogeochemical process modeling could be a question of interest to both communities. Outputs from biogeochemical process modeling may help constraining IP data interpretation, or can directly feed into SIP modeling. This can help better understand the underlying mechanisms driving IP signals. As suggested above with respect to the work of Mellage et al. (2018a,b) or Wu et al. (2011), using the IP data to calibrate a mechanistic model not only makes use of signals that are more directly related to the investigated process, but also provides in situ and time-continuous data that are normally hard to collect without sacrificial experiments.

Summary and Conclusions

Over the past decade, the induced polarization method has been used to monitor a variety of microbially mediated environmental processes and tested to directly characterize micro-organisms and biofilms. In addition, IP was found to be sensitive to plant systems, both in underground root systems and in aboveground stems.

Although the qualitative use of IP in biogeophysical studies is now established, several key points need to be researched in the near future to bring the IP method to its full potential. In the next ten years, we envision research to focus on gaining a better understanding of the polarization mechanisms

associated with the above IP signatures, and synthesize those findings into modeling frameworks for practical use. Particularly, more experimental and modeling work is necessary to understand the polarization mechanisms of single bacterial cells and even more complex biofilms. In order for laboratory experiments to be significant and help build comprehensive mechanistic models, more efforts need to be put in evaluating measurement uncertainty. Indeed, many experimental observations today are made on setups that are not replicated. It is thus hard to use such results as a basis for model development, as well as for convincing neighboring disciplines of the benefits of using the IP method. We believe that future laboratory experiments will systematically need to be replicated (measurement of at least triplicates) to better evaluate uncertainties in IP measurements. This applies to repetitions of measurements on the same setup as well as repetitions of the entire preparation protocol.

Recent modeling efforts suggest that bacterial cells are polarizable because of the presence of a polymeric brush layer that allows the development of an EDL around the bacterial cells. The polarization of biofilms is attributed to (i) bacterial cells with EDL, (ii) EPS that may behave like a polymer electrolyte, and (iii) non-cellular materials like clay grains that increase the surface conduction. Those explanations remain highly speculative and careful experimental studies are needed to verify the models. Regarding root structures, the polarization mechanisms are even more complex because the plant root systems are composed of multiple cell layers. The observations thus far have been explained by the presence of polarizable root cells inside the roots, with development of an EDL outside their plasma membrane and cross-membrane ion transport. More work is needed to understand how to scale-up these findings at a root system level and whether the interactions between the cells are playing an important role in the IP signal. The role of the porous medium should also be better considered when investigating both microbe-related and plant-related processes.

A major drawback is that IP is sensitive to multiple biological, physical and chemical processes in complex environments. Thus, a key challenge is the non-unique interpretation of the IP signal, due to detection of superimposed signatures of processes influencing the effective polarization. This can be overcome by several strategies that need to be tested in combination. Ideally, IP measurements should be coupled with direct biogeochemical measurements and interpreted jointly in mechanistic approaches.

Additionally, for plant root systems, indirect current injection could be combined with stem-based excitation methods to distinguish root polarization from the other soil polarization sources. Another possible strategy is to use multi-frequency (in FDIP) or full waveform (in TDIP) measurements to help differentiate the processes that have different relaxation frequencies. Besides, as biological processes are much more dynamic than other processes (e.g. soil textural changes or groundwater level variations), time-lapse measurements could help to distinguish between different contributions. Lastly, the development of experiments at an intermediate scale (lysimeter scale) is needed to study the IP sensitivity to heterogeneities in a controlled environment.

Apart from direct development of the IP method to biogeophysical studies in the future, both in the laboratory and in the field, we believe IP could be very useful if integrated in the experimental or modeling protocol of neighboring disciplines. IP could especially bridge the methodological gap in geomicrobiological studies, as it is non-destructive and possesses a good spatial and temporal resolution. It could also be used in studies of extracellular electron transfer to understand the fundamental mechanisms. Besides, IP could become a tool for plant physiologists to study plant root systems at various scales from the laboratory to the field, including the lysimeter scale. In addition, IP can be used to monitor tree stem activity in fully-grown trees, whichcould not be studied at smaller scales or by using destructive methods. To understand the methodological needs of these different neighboring research communities, it is crucial to encourage communication and interactions between the different scientific communities through research collaborations and joint symposiums and conferences. We believe that only such close partnerships will reveal the full potential of the IP method related to the biosphere.

Tables

Table 1: List of IP parameters used to understand the link between the polarization effects and the biogeochemical transformations in the subsurface

List of IP parameters

$\boldsymbol{\rho}^*$ $[\Omega.m]$ = complex electrical resistivity

$\boldsymbol{\sigma}^*$ $[S/m]$ = complex electrical conductivity

$$\sigma^* = 1/\rho^*$$

$$\sigma^* = \sigma^{'} + i\sigma^{''} = |\sigma^*|.e^{i\varphi}$$

$\boldsymbol{\sigma}^{'}$ $[S/m]$ = real part of electrical conductivity

$\boldsymbol{\sigma}^{''}$ $[S/m]$ = imaginary part of electrical conductivity

$|\boldsymbol{\sigma}^*|$ $[S/m]$ = magnitude/modulus of the complex electrical conductivity

$\boldsymbol{\varphi}$ $[rad]$ = phase shift or phase lag of the complex electrical conductivity

Cole-Cole model (Cole & Cole 1941) :

$$\sigma^* = \sigma_\infty + \frac{\sigma_0 - \sigma_\infty}{1 + (i\omega\tau_r)^c} = \sigma_\infty\left(1 - \frac{M_t}{1 + (i\omega\tau_r)^c}\right)$$

$\boldsymbol{c}$ [ ] = Cole-Cole model coefficient

$\boldsymbol{\sigma_0}$ $[S/m]$ = asymptotic low frequency conductivity

$\boldsymbol{\sigma_\infty}$ $[S/m]$ = asymptotic high frequency conductivity

$\boldsymbol{M_t}$ [ ] = total chargeability

$\boldsymbol{\tau_r}$ $[s]$ = characteristic relaxation time

$\boldsymbol{f_r}$ $[Hz]$ = characteristic relaxation frequency ($f_r = 1/2.\pi.\tau_r$)

Figures

Figure 1. (a) Conceptual diagram of a generalized electrical double layer (EDL) model of a bacterial cell. The cell envelope encapsulates the conductive cytoplasmic core and is made up of a plasma membrane and a cell wall. The cell wall consists of: (i) either a thin layer of peptidoglycan, and an outer membrane for gram-negative bacteria, or a thick peptidoglycan layer for gram-positive bacteria (Poortinga et al., 2002; Willey et al., 2014);and (ii) a charged, ion-permeable cell surface, denoted here as a *polymeric brush layer* (figure modified from Revil et al. (2012)).
(b) Potential distribution in the ion-permeable cell-surface (diagram content is modified from Poortinga et al. (2002)). (Note: the cell envelop structure presented here is meant to depict a generalized membrane for both gram-positive and -negative bacteria. The contribution to the IP effect is thought to be dominated by the charged functional groups in the ion-permeable cell-surface.)

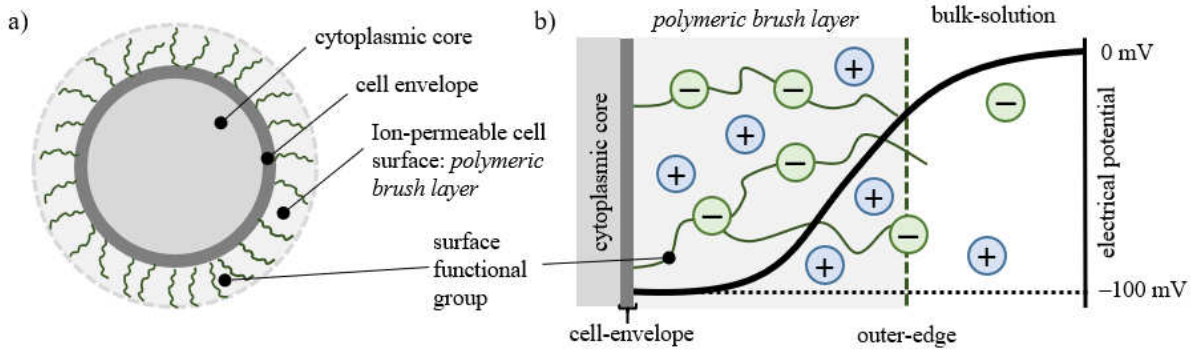

947 Figure 2: Conceptual diagram depicting Stern layer polarization tangential to a negatively charged
948 bacterial cell (modified from Mellage et al. (2018b)). Polarization of cells induces charge storage,
949 quantified as imaginary conductivity (σ") or normalized chargeability (m_n). The time-scale for ion back-
950 diffusion (i.e., the relaxation time, τ [s]) is governed by the effective length-scale or diameter (d) of the
951 polarizing particles, after Schwarz (1962). Surface diffusion, dependent on ionic mobility within the
952 cell EDL, is quantified by the effective-surface diffusion coefficient, D_s [$\mu m^2\ s^{-1}$].

953

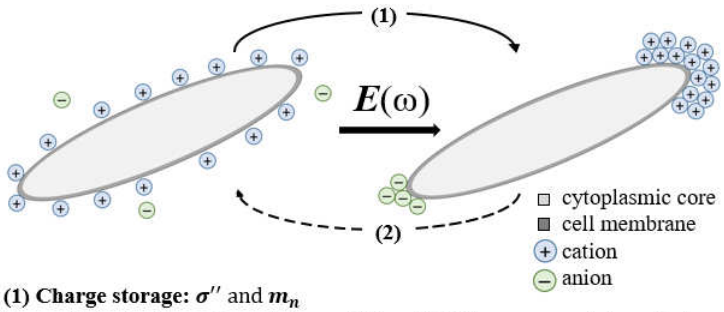

(1) Charge storage: σ'' and m_n
Tangential migration of counterions within cell EDL once current is applied

(2) Ion back-diffusion: $\tau = \frac{d^2}{8D_s}[s]$ (Schwarz, 1962)
Diffusion-controlled relaxation, back to equilibrium state, within the cell EDL

954

955

Figure 3: Electron transfer by: (left) direct contact between the insoluble electron donor/acceptor (black surface) and a redox-active component associated with the cell surface such as c-type cytochromes (OM c-cyt), (middle) the diffusion of soluble redox mediators (e.g. flavins, phenazines, and quinones), also known as electron shuttles, and (right) the production of elongated conductive pili or nanowires and redox cofactors (c-type cytochromes) within biofilms. (sequential electron-transfer self-exchange reactions) (Borole et al. 2011).

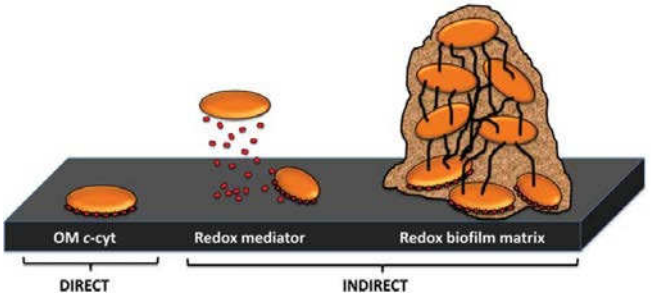

965 Figure 4: Microbially-driven processes that lead to enhanced IP signals through physical,chemical and
966 biological subsurface changes. The lighter grey arrow between "biological" and "IP signal" represent
967 the weaker influence of the direct biological markers compared to biologically-mediated physical and
968 chemical transformations. Modified from Atekwana and Slater (2009).

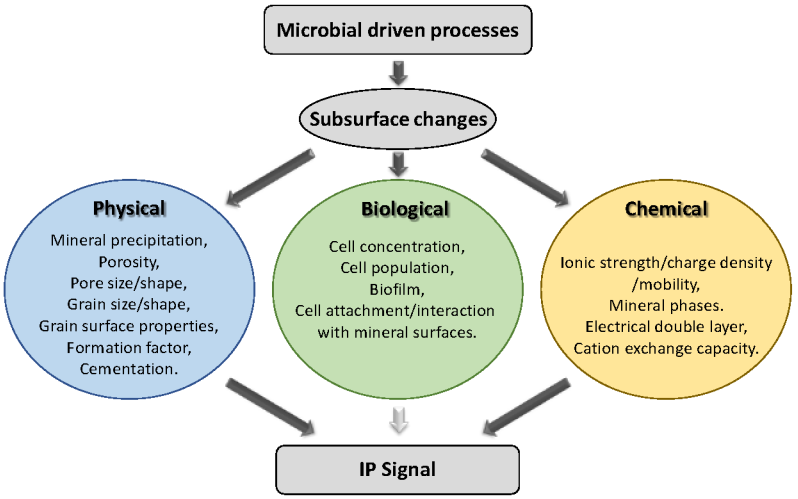

969
970

971

Figure 5: Conceptual diagram of ureolytically-driven calcium carbonate precipitation approach for remediation of ^{90}Sr contaminated geologic media. A. Microbially catalyzed hydrolysis of urea. B. Cation exchange and calcium carbonate precipitation. C. Continued precipitation of calcium carbonate (from Wu et al. (2011)).

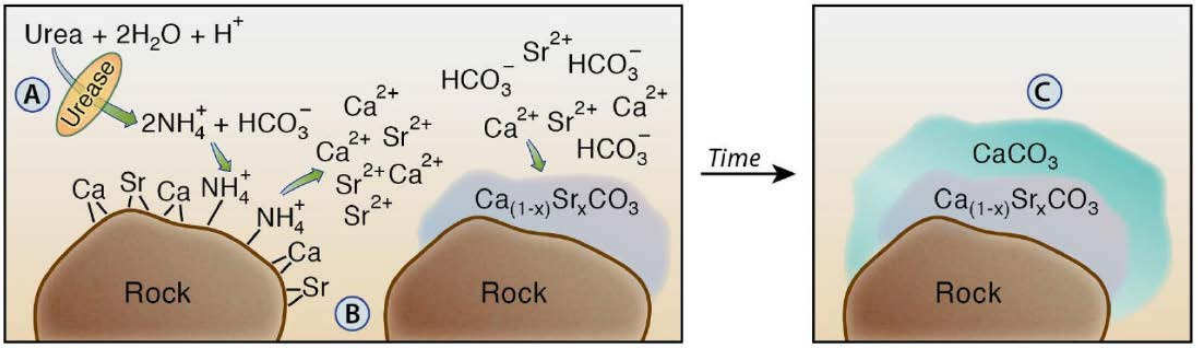

Figure 6: Average magnitude (left) and phase (right) of the complex electrical resistivity of an 8-day old Maize root determined from four-point SIP measurement on four root segments of living seedlings. Error bars indicate the standard deviation of the four measurements. The SIP measurements were made with a custom-made sample holder where both current and potential electrodes were connected with the root segment using a conductive gel. (Ehosioke et al. 2018).

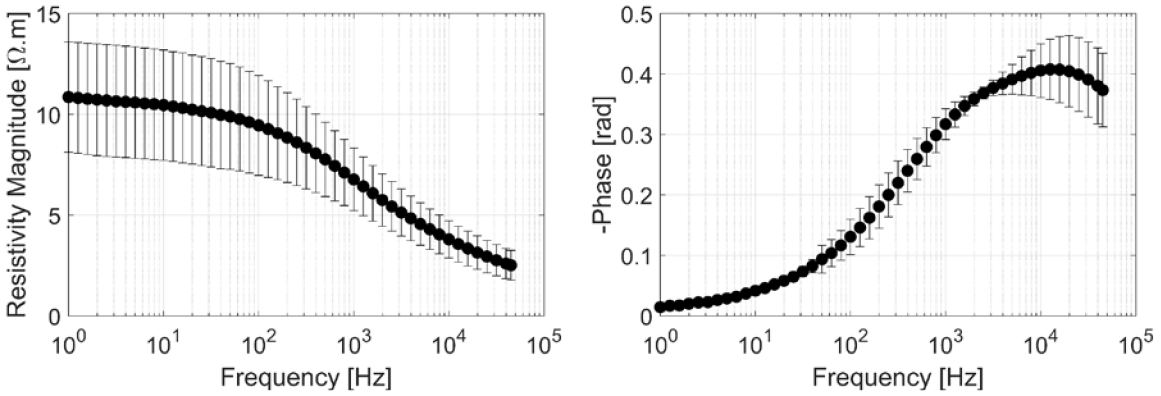

Figure 7: Conceptual model at the root cell scale as proposed by Weigand and Kemna (2019) relating ion uptake fluxes to the strength of electrochemical (EDL) polarizability based on the electric potential distribution across a root cell membrane (Kinraide 2001; Kinraide and Wang 2010; Wang et al. 2011). Lower negativity of outer surface potential (φ_0) at the plasma membrane (PM) (a) left scenario vs. b) right scenario) corresponds with, on the one hand, increased surface-to-surface transmembrane potential difference ($\Delta\varphi_{PM}$) and enhanced cation flux (j_{up}) into the cell and, on the other hand, decreased surface charge density of the membrane and decreased polarizability of the EDL at the outer surface of the membrane due to an external electric field, similar to the behavior of electrochemical polarization around metallic particles.

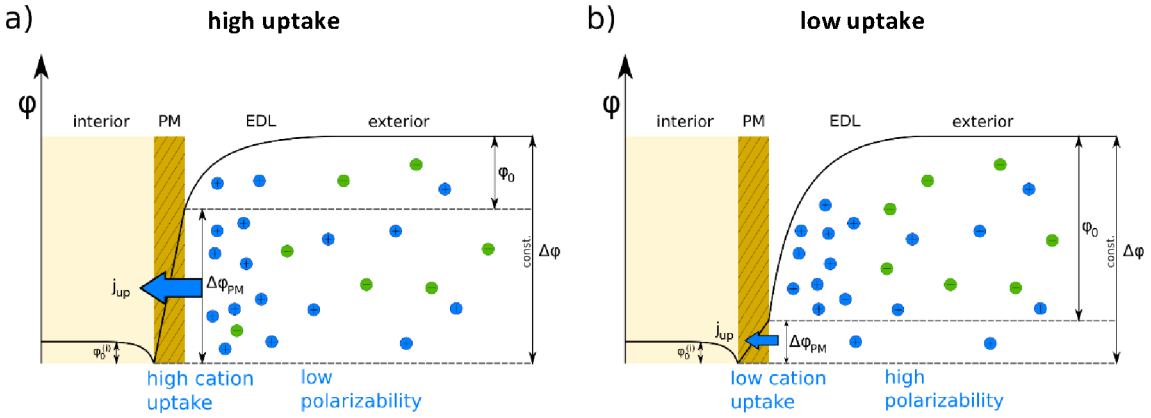

Figure 8: Known causes of the IP signature of dead wood and living trees and application domains for both materials. Causes at the junction of both circles are common to both dead wood and living trees.

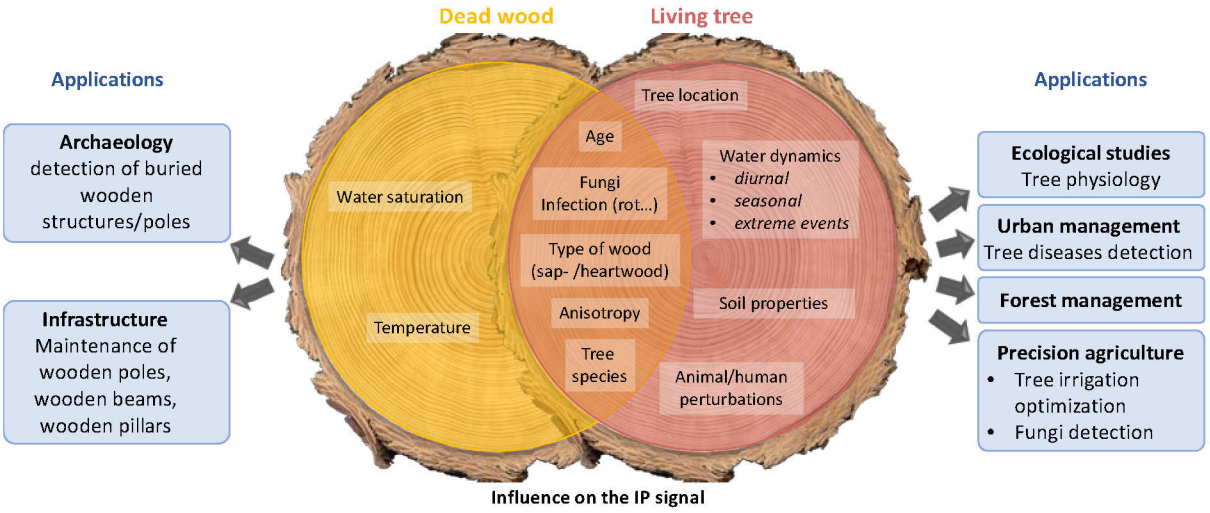

Figure 9: Conceptual model of the next steps needed in research projects on IP and biogeophysics to be able to use the IP method as a tool to characterize biological processes at various scales from the laboratory to the field scale. Solid arrows represent the primary target for the study: for example, laboratory studies are aiming to build a modeling framework linking the IP signals with the biological processes. Dashed arrows are representing the secondary goals that could be achieved as well; for example, modeling framework could be re-applied in laboratory biogeochemical experimentations where IP is used as a laboratory tool.

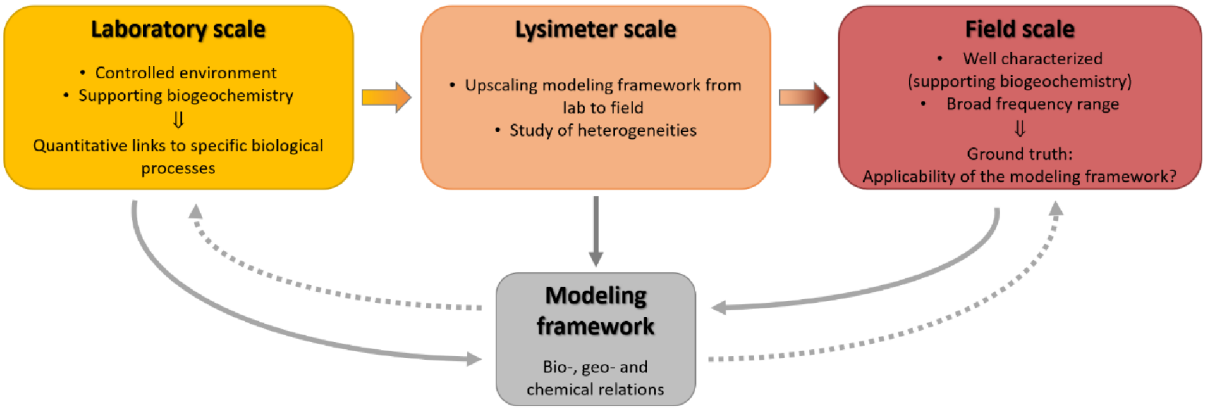

Figure 10: Conceptual joint interpretation scheme. Models, such as reactive transport models (RTMs) use biological, chemical and physical datasets available (low spatial and temporal resolutions) to estimate biological, physical or chemical properties with higher resolutions. Comparison with IP measurements can help develop petrophysical relationships between these two types of datasets. As IP data have better spatial and temporal resolutions than the other datasets used in the RTMs, they can be used to calibrate these models.

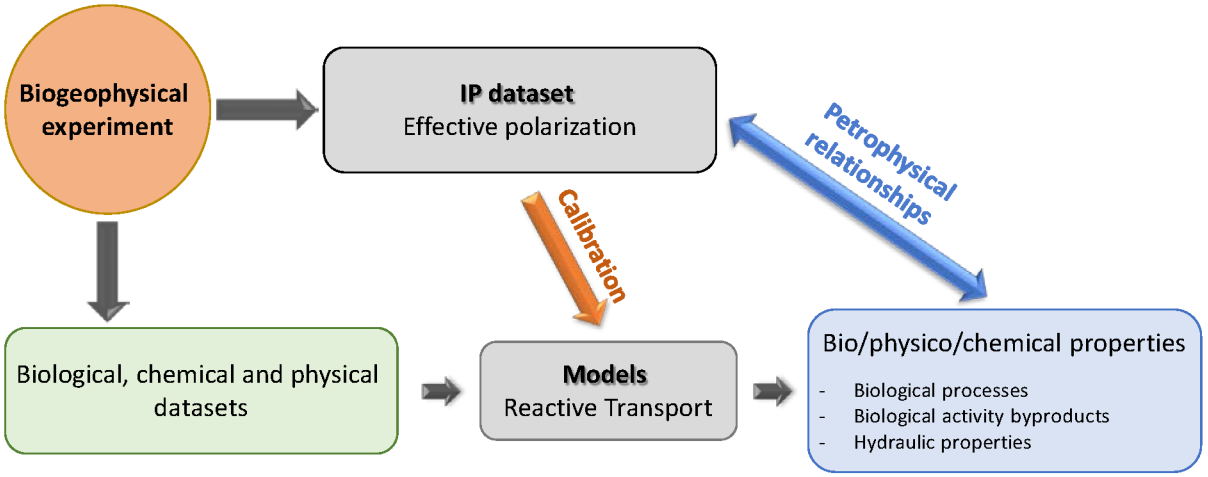

Figure legends

Figure 1: . (a) Conceptual diagram of a generalized electrical double layer (EDL) model of a bacterial cell. The cell envelope encapsulates the conductive cytoplasmic core and is made up of a plasma membrane and a cell wall. The cell wall consists of: (i) either a thin layer of peptidoglycan, and an outer membrane for gram-negative bacteria, or a thick peptidoglycan layer for gram-positive bacteria (Poortinga et al., 2002; Willey et al., 2014);and (ii) a charged, ion-permeable cell surface, denoted here as a *polymeric brush layer* (figure modified from Revil et al. (2012)).
(b) Potential distribution in the ion-permeable cell-surface (diagram content is modified from Poortinga et al. (2002)). (Note: the cell envelop structure presented here is meant to depict a generalized membrane for both gram-positive and -negative bacteria. The contribution to the IP effect is thought to be dominated by the charged functional groups in the ion-permeable cell-surface.)

Figure 2: Conceptual diagram depicting Stern layer polarization tangential to a negatively charged bacterial cell (modified from Mellage et al. (2018b)). Polarization of cells induces charge storage, quantified as imaginary conductivity (σ'') or normalized chargeability (m_n). The time-scale for ion back-diffusion (i.e., the relaxation time, τ [s]) is governed by the effective length-scale or diameter (d) of the polarizing particles, after Schwarz (1962). Surface diffusion, dependent on ionic mobility within the cell EDL, is quantified by the effective-surface diffusion coefficient, D_s [$\mu m^2\ s^{-1}$].

Figure 3: Electron transfer by: (left) direct contact between the insoluble electron donor/acceptor (black surface) and a redox-active component associated with the cell surface such as c-type cytochromes (OM c-cyt), (middle) the diffusion of soluble redox mediators (e.g. flavins, phenazines, and quinones), also known as electron shuttles, and (right) the production of elongated conductive pili or nanowires and redox cofactors (c-type cytochromes) within biofilms. (sequential electron-transfer self-exchange reactions) (Borole et al. 2011).

Figure 4: Microbially-driven processes that lead to enhanced IP signals through physical,chemical and biological subsurface changes. The lighter grey arrow between "biological" and "IP signal" represent the weaker influence of the direct biological markers compared to biologically-mediated physical and chemical transformations. Modified from Atekwana and Slater (2009).

Figure 5: Conceptual diagram of ureolytically-driven calcium carbonate precipitation approach for remediation of ^{90}Sr contaminated geologic media. A. Microbially catalyzed hydrolysis of urea. B. Cation exchange and calcium carbonate precipitation. C. Continued precipitation of calcium carbonate (from Wu et al. 2011).

Figure 6: Average magnitude (left) and phase (right) of the complex electrical resistivity of an 8-day old Maize root determined from four-point SIP measurement on four root segments of living seedlings. Error bars indicate the standard deviation of the four measurements. The SIP measurements were made with a custom-made sample holder where both current and potential electrodes were connected with the root segment using a conductive gel. (Ehosioke et al. 2018).

Figure 7: Conceptual model at the root cell scale as proposed by Weigand and Kemna (2019) relating ion uptake fluxes to the strength of electrochemical (EDL) polarizability based on the electric potential distribution across a root cell membrane (Kinraide 2001; Kinraide and Wang 2010; Wang et al. 2011). Lower negativity of outer surface potential (φ_0) at the plasma membrane (PM) (a) left scenario vs. b) right scenario) corresponds with, on the one hand, increased surface-to-surface transmembrane

potential difference ($\Delta\varphi_{PM}$) and enhanced cation flux (j_{up}) into the cell and, on the other hand, decreased surface charge density of the membrane and decreased polarizability of the EDL at the outer surface of the membrane due to an external electric field, similar to the behavior of electrochemical polarization around metallic particles.

Figure 8: Known causes of the IP signature of dead wood and living trees and application domains for both materials. Causes at the junction of both circles are common to both dead wood and living trees.

Figure 9: Conceptual model of the next steps needed in research projects on IP and biogeophysics to be able to use the IP method as a tool to characterize biological processes at various scales from the laboratory to the field scale. Solid arrows represent the primary target for the study: for example, laboratory studies are aiming to build a modeling framework linking the IP signals with the biological processes. Dashed arrows are representing the secondary goals that could be achieved as well; for example, modeling framework could be re-applied in laboratory biogeochemical experimentations where IP is used as a laboratory tool.

Figure 10: Conceptual joint interpretation scheme. Models, such as reactive transport models (RTMs) use biological, chemical and physical datasets available (low spatial and temporal resolutions) to estimate biological, physical or chemical properties with higher resolutions. Comparison with IP measurements can help develop petrophysical relationships between these two types of datasets. As IP data have better spatial and temporal resolutions than the other datasets used in the RTMs, they can be used to calibrate these models.

References

Abdel Aal G. Z., Atekwana E. A., Slater L. D., and Atekwana E. A. 2004. Effects of microbial processes on electrolytic and interfacial electrical properties of unconsolidated sediments. Geophysical Research Letters, 31(12), L12505.

Abdel Aal G. Z., Atekwana E. A., Radzikowski S., and Rossbach, S. 2009. Effect of bacterial adsorption on low frequency electrical properties of clean quartz sands and iron-oxide coated sands. Geophysical Research Letters, 36(4), L04403.

Abdel Aal G. Z., Atekwana E. A., and Atekwana E. A. 2010. Effect of bioclogging in porous media on complex conductivity signatures. Journal of Geophysical Research: Biogeosciences, 115(G3).

Albrecht R., Gourry J. C., Simonnot M.-O., and Leyval C. 2011. Complex conductivity response to microbial growth and biofilm formation on phenanthrene spiked medium. Journal of Applied Geophysics, 75(3), 558-564.

Al Hagrey S. A. 2006. Electrical resistivity imaging of tree trunks, Near Surface Geophysics, 4(3), 179-187.

Anneser B., Einsiedl F., Meckenstock R. U., Richters L., Wisotzky F., and Griebler C. 2008. High-resolution monitoring of biogeochemical gradients in a tar oil-contaminated aquifer. Applied Geochemistry, 23(6), 1715-1730.Atekwana, E. A., Sauck, W. A., & Werkema, D. D. 2000. Investigations of geoelectrical signatures at a hydrocarbon contaminated site. Journal of Applied Geophysics, *44*(2), 167–180. https://doi.org/10.1016/S0926-9851(98)00033-0.

Atekwana E. A., Atekwana E. A., Rowe R. S., Werkema D. D., and Legall F. D. 2004a. The relationship of total dissolved solids measurements to bulk electrical conductivity in an aquifer contaminated with hydrocarbon. Journal of Applied Geophysics. 56(4), 281-294.

Atekwana E. A., Werkema D. D., Duris J. W., Rossbach S., Atekwana E. A., Sauck W. A., et al. 2004b. In-situ apparent conductivity measurements and microbial population distribution at a hydrocarbon-contaminated site, *69*(1), 56–63.Atekwana, E. A., and Slater, L. D. 2009. Biogeophysics: A new frontier in earth science research. Reviews of Geophysics, 47(4), RG4004.

Atekwana E. A., Atekwana E. A. 2010. Geophysical Signatures of Microbial Activity at Hydrocarbon Contaminated Sites: A Review. Surv. Geophys. 31, 247–283. https://doi.org/10.1007/s10712-009-9089-8

Avis T.J., Gravel V., Antoun H., Tweddell R.J. 2008. Multifaceted beneficial effects of rhizosphere microorganisms on plant health and productivity. Soil Biol. Biochem. 40, 1733–1740. https://doi.org/10.1016/J.SOILBIO.2008.02.013

Babauta J., Renslow R., Lewandowski Z., and Beyenal H. 2012. Electrochemically active biofilms: facts and fiction. A review. Biofouling, 28(8), 789-812.

Barsoukov E., Macdonald J.R. 2018. Impedance spectroscopy : theory, experiment, and applications., 3rd ed.

Bartholomew J. W., & Mittwer T. 1952. The gram stain. Bacteriological reviews, 16(1), 1.

Baszkin A. and Norde W., 1999. Physical chemistry of biological interfaces. CRC Press. 823 p. ISBN: 0-8247-7581-3.Benedetti M., Van Riemsdijk W., and Koopal L. 1996. Humic substances considered as a heterogeneous Donnan gel phase. Environmental Science & Technology, 30(6), 1805-1813.

Bera T.K., 2014. Bioelectrical Impedance Methods for Noninvasive Health Monitoring: A Review. J. Med. Eng. 2014, 1–28. https://doi.org/10.1155/2014/381251

Berlanga M., and Guerrero R. 2016. Living together in biofilms: the microbial cell factory and its biotechnological implications. Microbial cell factories, 15(1), 165.

Bermejo J. L., Sauck W. A., & Atekwana E. A. 1997. Geophysical Discovery of a New LNAPL Plume at the Former Wurtsmith AFB, Oscoda, Michigan. Ground Water Monitoring & Remediation, 17(4), 131–137. https://doi.org/10.1111/j.1745-6592.1997.tb01273.x

Beyenal H., and Babauta J. T. 2015, Biofilms in bioelectrochemical systems: from laboratory practice to data interpretation, John Wiley & Sons.

Bieker D and Rust S. 2010. Non-destructive estimation of sapwood and heart-wood width in Scots pine (Pinus sylvestris L.), Silva Fennica, 44(2), 267–273.

Bieker D., Kehr R., Weber G. and Rust S. 2010. Non-destructive monitoring of early stages of white rot by Trametes versicolor in Fraxinus excelsior. Annals of Forest Science, 67(2), 210, 1-7.

Binley A., and Kemna A. 2005. DC Resistivity and Induced Polarization Methods. In Hydrogeophysics, 129–56. Dordrecht: Springer Netherlands. https://doi.org/10.1007/1-4020-3102-5_5.

Bodelier P.L.E., Dedysh S.N. 2013. Microbiology of wetlands. Front. Microbiol. 4, 79. https://doi.org/10.3389/fmicb.2013.00079

Bond D. R., Strycharz-Glaven S. M., Tender L. M., and Torres C. I. 2012. On electron transport through Geobacter biofilms. ChemSusChem. 5(6), 1099-1105.

Borole A. P., Reguera G., Ringeisen B., Wang Z.-W., Feng Y., and Kim B. H. 2011. Electroactive biofilms: current status and future research needs. Energy & Environmental Science, 4(12), 4813-4834.

Brandt M. and Rinn F. 1989. Eine Übersicht über Verfahren zur Stammfäulediagnose, Holz-Zentralblatt, 80, 1268-1270.

Breede K., A. Kemna O. Esser E. Zimmermann H. Vereecken and Huisman J.A. 2012. Spectral induced polarization measurements on variably saturated sand-clay mixtures. Near Surf. Geophys. 10(6):479-489.

Bücker M., and Hördt A. 2013. Analytical modelling of membrane polarization with explicit parametrization of pore radii and the electrical double layer. Geophysical Journal International, 194(2): 804–813.

Bücker M., Flores-Orozco A. F., Hördt A., and Kemna A. 2017. An analytical membrane-polarization model to predict the complex conductivity signature of immiscible liquid hydrocarbon contaminants. Near Surface Geophysics, 15(6), 547–562. https://doi.org/10.3997/1873-0604.2017051

Bücker M., Flores-Orozco A., and Kemna A. 2018. Electrochemical polarization around metallic particles – Part 1: The role of diffuse-layer and volume-diffusion relaxation. Geophysics, 83(4), E203-E217.

Bücker M., Undorf S., Flores-Orozco A., and Kemna A. 2019. Electrochemical polarization around metallic particles – Part 2: The role of diffuse surface charge. Geophysics, 84(2), E57-E73.

Cao Y., Repo T., Silvennoinen R., Lehto T., and Pelkonen P. 2011. Analysis of the willow root system by electrical impedance spectroscopy. Journal of Experimental Botany, 62(1), 351–358.

Carstensen E., and Marquis R. 1968. Passive electrical properties of microorganisms: III. Conductivity of isolated bacterial cell walls. Biophysical journal, 8(5), 536-548.

Cassiani G., Binley A., Kemna A., Wehrer M., Flores-Orozco A., Deiana R., et al. 2014. Noninvasive characterization of the Trecate (Italy) crude-oil contaminated site: links between contamination and geophysical signals. Environmental Science and Pollution Research, 21(15), 8914–8931. https://doi.org/10.1007/s11356-014-2494-7

Cassiani G., Boaga J., Vanella D., Perri M.T., and Consoli S. 2015. Monitoring and modelling of soil–plant interactions: the joint use of ERT, sap flow and eddy covariance data to characterize the volume of an orange tree root zone. Hydrology and Earth System Sciences, 19(5), 2213 - 2225.

Chloupek O. 1972. The relationship between electrical capacitance and some other parameters of plant root. Biologia Plantarum, 14(3), 227–230.

Chloupek O. 1977. Evaluation of the size of plant's root-system using its electrical capacitance. Plant and Soil, 48(2), 525-532.

Claessens J., Behrends T., and Van Cappellen P. 2004. What do acid-base titrations of live bacteria tell us? A preliminary assessment. Aquatic Sciences, 66(1), 19-26.

Cole K. S., and Cole R. H. 1941. Dispersion and absorption in dielectrics I. Alternating current characteristics. The Journal of Chemical Physics, 9(4), 341-351.

Colwell F. S., Smith R. W., Ferris F. G., Reysenbach A.-L., Fujita Y., Tyler T. L., et al. 2005. Microbial Mediated Subsurface Calcite Precipitation for Removal of Hazardous Divalent Cations: Microbial Activity, Molecular Biology, and Modeling. In E. Berkey & T. Zachary (Eds.), Subsurface Contamination Remediation: Accomplishments of the Environmental Management Science Program (Vol. 904, pp. 117–137). Washington: American Chemical Society.

Dahlin T. and Leroux V. 2012. Improvement in time-domain induced polarization data quality with multi-electrode systems by separating current and potential cables. Near Surf. Geophys., 10(6), 545–565. doi:10.3997/1873-0604.2012028

Dahlin T., Leroux V. and Nissen J. 2002. Measuring techniques in induced polarisation imaging. J. Appl. Geophys., 50(3), 279–298. doi:10.1016/S0926-9851(02)00148-9

Dahlin T., & Zhou B. 2006. Multiple-gradient array measurements for multichannel 2D resistivity imaging. Near Surface Geophysics, 4(2), 113-123.

Dalton F. N. 1995. In-situ root extent measurements by electrical capacitance methods. Plant and Soil 173(1), 157-165.

Davis C. A., Atekwana E. A., Atekwana E. A., Slater L. D., Rossbach S., and Mormile M. R. 2006. Microbial growth and biofilm formation in geologic media is detected with complex conductivity measurements. Geophysical Research Letters, 33(18), L18403.

Davis C. A., Pyrak-Nolte L. J., Atekwana E. A., Werkema D. D., and Haugen M. E. 2010. Acoustic and electrical property changes due to microbial growth and biofilm formation in porous media. Journal of Geophysical Research: Biogeosciences. 115(G3).

Deceuster J., and Kaufmann O. 2012. Improving the delineation of hydrocarbon-impacted soils and water through induced polarization (IP) tomographies: A field study at an industrial wasteland. Journal of Contaminant Hydrology, 136, 25–42. https://doi.org/10.1016/j.jconhyd.2012.05.003

DeJong J. T., Mortensen B. M., Martinez B. C., and Nelson D. C. 2010. Bio-mediated soil improvement. Ecological Engineering, 36(2), 197–210. https://doi.org/10.1016/j.ecoleng.2008.12.029

DeJong J. t., Soga K., Kavazanjian E., Burns S., Van Paassen L. A., Al Qabany A., et al. 2013. Biogeochemical processes and geotechnical applications: progress, opportunities and challenges. Géotechnique, 63(4), 287–301. https://doi.org/10.1680/geot.SIP13.P.017

Dhami N. K., Reddy M. S., and Mukherjee A. 2013. Biomineralization of calcium carbonates and their engineered applications: a review. Frontiers in Microbiology, 4, 314. https://doi.org/10.3389/fmicb.2013.00314

Dietrich R. C., Bengough A. G., Jones H. G., and White P. J. 2012. A new physical interpretation of plant root capacitance. Journal of Experimental Botany, 63(17), 6149–6159.

Dietrich R. C., Bengough A.G, Jones H.G., and White P.J. 2013. Can root electrical capacitance be used to predict root mass in soil? Annals of Botany, 112(2), 457–464.

Dominguez-Benetton X., Sevda S., Vanbroekhoven K., and Pant D. 2012. The accurate use of impedance analysis for the study of microbial electrochemical systems. Chemical Society Reviews. 41(21), 7228-7246.

Donlan R. M. 2002. Biofilms: microbial life on surfaces. Emerging infectious diseases. 8(9), 881.

Ehosioke S., Garré S., Kremer T., Rao S., Kemna A., Huisman J. A., Zimmermann E., Javaux M., and Nguyen F. 2018. A new method for characterizing the complex electrical properties of root segments. Abstract (Oral) presented at the ISRR-10 "Exposing the hidden half", Ma'ale HaHamisha, Israel, 08.07.2018-12.07.2018.

Fang C., Smith P., Smith J.U., Moncrieff J.B., 2005. Incorporating microorganisms as decomposers into models to simulate soil organic matter decomposition. Geoderma 129, 139–146. https://doi.org/10.1016/J.GEODERMA.2004.12.038

Fernandez P. M., Binley A., Bloem E., and French H. K. 2018. Laboratory spectral induced polarisation signatures associated with iron and manganese oxide dissolution because of anaerobic degradation. Journal of Contaminant Hydrology, 221, 1-10. https://doi.org/10.1016/j.jconhyd.2018.12.002

Fiandaca G., Ramm J., Binley A., Gazoty A., Christiansen A. V., and Auken E. 2013. Resolving Spectral Information from Time Domain Induced Polarization Data through 2-D Inversion. Geophysical Journal International, 192(2). 631–646. https://doi.org/10.1093/gji/ggs060.

Fiandaca G., Auken E., Vest Christiansen A., and Gazoty A. 2012. Time-Domain-Induced Polarization: Full-Decay Forward Modeling and 1D Laterally Constrained Inversion of Cole-Cole Parameters. Geophysics, 77 (3), E213-E225. https://doi.org/10.1190/geo2011-0217.1.

Flores-Orozco A., Williams K. H., Long P. E., Hubbard S. S., and Kemna A. 2011. Using complex resistivity imaging to infer biogeochemical processes associated with bioremediation of an uranium-contaminated aquifer, Journal of Geophysical Research: Biogeosciences. 116(G3), 2156–2206, doi: 10.1029/2010JG001591.

Flores-Orozco A., Kemna A., Oberdörster C., Zschornack L., Leven C., Dietrich P., and Weiss H. 2012. Delineation of subsurface hydrocarbon contamination at a former hydrogenation plant using spectral induced polarization imaging. Journal of Contaminated Hydrology, 136, 131-144.

Flores-Orozco A., Williams K.H. and Kemna A. 2013. Time-lapse spectral induced polarization imaging of stimulated uranium bioremediation. Near Surface Geophysics, 11(5), 531–544. https://doi.org/10.3997/1873-0604.2013020.

Flores-Orozco A., Velimirovic M., Tosco T., Kemna A., Sapion H., Klaas N., et al. 2015. Monitoring the Injection of Microscale Zerovalent Iron Particles for Groundwater Remediation by Means of Complex Electrical Conductivity Imaging. Environmental Science & Technology, 49(9), 5593–5600. https://doi.org/10.1021/acs.est.5b00208

Flores-Orozco A., Gallistl J., Bücker M., and Williams K. H. 2018. Decay curve analysis for data error quantification in time-domain induced polarization imaging. Geophysics, 83(2), E75 – E86

Foster K.R., Schwan H.P. 1989. Dielectric properties of tissues and biological materials: a critical review. Crit. Rev. Biomed. Eng. 17, 25–104.

Fröhlich H. 1975. The extraordinary dielectric properties of biological materials and the action of enzymes. Proc. Natl. Acad. Sci. U. S. A. 72, 4211–5. https://doi.org/10.1073/pnas.72.11.4211

Fujita Y., Taylor J. L., Gresham T. L. T., Delwiche M. E., Colwell F. S., Mcling T. L., et al. 2008. Stimulation of Microbial Urea Hydrolysis In Groundwater To Enhance Calcite Precipitation. Environmental Science & Technology, 42(8), 3025–3032. https://doi.org/10.1021/es702643g

Fujita Y., Taylor J. L., Wendt L. M., Reed D. W., and Smith R. W. 2010. Evaluating the potential of native ureolytic microbes to remediate a 90Sr contaminated environment. Environmental Science & Technology, 44(19), 7652–7658. https://doi.org/10.1021/es101752p

Gallistl J., Weigand M., Stumvoll M., Ottowitz D., Glade T. and Flores-Orozco A., 2018. Delineation of subsurface variability in clay-rich landslides through spectral induced polarization imaging and electromagnetic methods. Engineering Geology, 245, 292-308.

Garré S., Javaux M., Vanderborght J., Pagès L., and Vereecken H. 2011. Three-dimensional electrical resistivity tomography to monitor root zone water dynamics. Vadose Zone Journal, 10(1), 412-424.

Ghestem M., Sidle R.C., Stokes A. 2011. The Influence of Plant Root Systems on Subsurface Flow: Implications for Slope Stability. Bioscience 61, 869–879. https://doi.org/10.1525/bio.2011.61.11.6

Grayston S.J., Vaughan D., Jones D. 1997. Rhizosphere carbon flow in trees, in comparison with annual plants: the importance of root exudation and its impact on microbial activity and nutrient availability. Appl. Soil Ecol. 5, 29–56. https://doi.org/10.1016/S0929-1393(96)00126-6

Guyot A., Ostergaard K. T., Lenkopane M., Fan J. and Lockington D.A. 2013. Using electrical resistivity tomography to differentiate sapwood from heartwood: application to conifers. Tree Physiology, 33(2), 187-194.

Hammes F., Boon N., de Villiers J., Verstraete W., and Siciliano S. D. 2003. Strain-Specific Ureolytic Microbial Calcium Carbonate Precipitation. Applied and Environmental Microbiology, 69(8), 4901–4909. https://doi.org/10.1128/AEM.69.8.4901-4909.2003

Heenan J., Porter A., Ntarlagiannis D., Young L. Y., Werkema D. D., and Slater L. D. 2013. Sensitivity of the spectral induced polarization method to microbial enhanced oil recovery processes. Geophysics, 78(5), E261–E269. https://doi.org/10.1190/geo2013-0085.1

Heenan J., Slater L. D., Ntarlagiannis D., Atekwana E. A., Fathepure B. Z., Dalvi S., et al. 2015. Electrical resistivity imaging for long-term autonomous monitoring of hydrocarbon degradation: Lessons from the Deepwater Horizon oil spill. Geophysics, 80(1), B1–B11. https://doi.org/10.1190/geo2013-0468.1

Herbert-Guillou D., Tribollet B., Festy D., and Kiéné L. 1999. In situ detection and characterization of biofilm in waters by electrochemical methods. Electrochimica Acta. 45(7), 1067-1075.

Holder D., 2004. Electrical Impedance Tomography : Methods, History and Applications. CRC Press, Boca Raton . https://doi.org/10.1201/9780367801595

Humphries J., Xiong L., Liu J., Prindle A., Yuan F., Arjes H. A., et al. 2017. Species-independent attraction to biofilms through electrical signaling. Cell. 168(1-2), 200-209.

Johansson S., Fiandaca G., and Dahlin T. 2015. Influence of non-aqueous phase liquid configuration on induced polarization parameters: Conceptual models applied to a time-domain field case study. Journal of Applied Geophysics, 123, 295–309. https://doi.org/10.1016/j.jappgeo.2015.08.010

Kanematsu H., and Barry D. M. (Eds.) 2015. Biofilm and materials science. Springer.

Kappler A., Emerson D., Edwards K., Amend J., Gralnick J., Grathwohl P., et al. 2005. Microbial activity in biogeochemical gradients–new aspects of research. Geobiology, 3(3), 229-233.

Kelter M., Huisman J. A., Zimmermann E., and Vereecken H. 2018. Field evaluation of broadband spectral electrical imaging for soil and aquifer characterization. Journal of Applied Geophysics, 159, 484-496.

Kemna A., Vanderborght J., Kulessa B. and Vereecken H. 2002. Imaging and characterization of subsurface solute transport using electrical resistivity tomography (ERT) and equivalent transport models. Journal of Hydrology, 267(3-4), 125-146.

Kemna A., Binley A., and Slater L. 2004. Crosshole IP imaging for engineering and environmental applications. Geophysics, 69(1), 97–107. https://doi.org/10.1190/1.1649379

Kemna A., Huisman J. A., Zimmermann E., Martin R., Zhao Y., Treichel A., Flores-Orozco A., and Fechner T. 2014. Broadband Electrical Impedance Tomography for Subsurface Characterization Using Improved Corrections of Electromagnetic Coupling and Spectral Regularization. In Tomography of the Earth's Crust: From Geophysical Sounding to Real-Time Monitoring (pp. 1-20). Springer, Cham. https://doi.org/10.1007/978-3-319-04205-3_1.

Kendall W. A., Peferson G.A., and Hill R.R. 1982. Root size estimates of red clover and alfalfa based on electrical capacitance and root diameter measurements. Grass and Forage Science, 37(3): 253–256.

Kessouri P., Johnson T. C., Day-Lewis F. D., Slater L. D., Ntarlagiannis D. and Johnson C. D. 2016. Soil and groundwater VOCs contamination: How can electrical geophysical measurements help assess

post-bioremediation state? Abstract (Oral) presented at the 49th annual Fall Meeting of the American Geophysical Union, San Francisco (USA), 12.12.2016 -13.12.2016.

Kettridge N., Comas X., Baird A., Slater L. D., Strack M., Thompson D., et al. 2008. Ecohydrologically important subsurface structures in peatlands revealed by ground-penetrating radar and complex conductivity surveys. Journal of Geophysical Research: Biogeosciences, 113(G4).

Kimak C., Ntarlagiannis D., Slater L. D., Atekwana E. A., Beaver C. L., Rossbach S., et al. 2019. Geophysical monitoring of hydrocarbon biodegradation in highly conductive environments. Journal of Geophysical Research: Biogeosciences. https://doi.org/10.1029/2018JG004561

Kinniburgh D. G., Milne C. J., Benedetti M. F., Pinheiro J. P., Filius J., Koopal L. K., and Van Riemsdijk W. H. 1996. Metal ion binding by humic acid: application of the NICA-Donnan model. Environmental Science & Technology, 30(5), 1687-1698.

Kinraide T. B. 2001. Ion fluxes considered in terms of membrane-surface electrical potentials. Australian Journal of Plant Physiology, 28(7), 607-618.

Kinraide T.B., and Wang P. 2010. The surface charge density of plant cell membranes (σ): an attempt to resolve conflicting values for intrinsic σ. Journal of Experimental Botany, 61(9), 2507-2518.

Konhauser, K., 2007. Introduction to geomicrobiology. Blackwell Publishing Ltd.

Koopal L., Van Riemsdijk W., De Wit J., and Benedetti M. 1994. Analytical isotherm equations for multicomponent adsorption to heterogeneous surfaces. Journal of Colloid and Interface Science, 166(1), 51-60.

Lamers L.P.M., van Diggelen J.M.H., Op den Camp H.J.M., Visser E.J.W., Lucassen E.C.H.E.T., Vile M.A., Jetten M.S.M., Smolders A.J.P., Roelofs J.G.M., 2012. Microbial Transformations of Nitrogen, Sulfur, and Iron Dictate Vegetation Composition in Wetlands: A Review. Front. Microbiol. 3, 156. https://doi.org/10.3389/fmicb.2012.00156

Lehmann, J., Kleber, M., 2015. The contentious nature of soil organic matter. Nature 528, 60–68. https://doi.org/10.1038/nature16069

Li L., Maher K., Navarre-Sitchler A., Druhan J., Meile C., Lawrence C., et al. 2017. Expanding the role of reactive transport models in critical zone processes. Earth-science reviews, 165, 280-301.

Logan B. E., and Regan J. M. 2006. Microbial fuel cells - challenges and applications, edited, ACS Publications.

Malvankar N. S., Mester T., Tuominen M. T., and Lovley D. R. 2012. Supercapacitors based on c-type cytochromes using conductive nanostructured networks of living bacteria. ChemPhysChem. 13(2), 463-468.

Marinsky J. A., Lin F. G., and Chung K. S. 1983. A simple method for classification of the physical state of colloidal and particulate suspensions encountered in practice. The Journal of Physical Chemistry, 87(16), 3139-3145.

Martin T., 2012. Complex resistivity measurements on oak. European Journal of Wood and Wood Products, 70(1-3), 45-53.

Martin T. and Günther T. 2013. Complex Resistivity Tomography (CRT) for fungus detection on standing oak trees. European Journal of Forest Research ,132(5), 1-12.

Martin T., Nordsiek S. and Weller A. 2015. Low-Frequency Impedance Spectroscopy of Wood. Journal of Research in Spectroscopy, 2015. Article ID 910447. DOI: 10.5171/2015.910447

Mary B., Abdulsamad F., Saracco G., Peyras L., Vennetier M., Mériaux P., and Camerlynck C. 2017. Improvement of coarse root detection using time and frequency induced polarization: from laboratory to field experiments. Plant and Soil, 417(1-2), 243–259.

Mary B., Peruzzo L., Boaga J., Schmutz M., Wu Y., Hubbard S. S., and Cassiani G. 2018. Small scale characterization of vine plant root water uptake via 3D electrical resistivity tomography and Mise-à-la-Masse method. Hydrology and Earth System Sciences, 22(10), 5427-5444. doi:10.5194/hess-2018-238.

Maineult A., D. Jougnot and Revil A. 2018. Variations of petrophysical properties and spectral induced polarization in response to drainage and imbibition: a study on a correlated random tube network. Geophys. J. Int. 212, 1398-1411. http://dx.doi.org/10.1093/gji/ggx474

Mellage A., Holmes A. B., Linley S., Vallée L., Rezanezhad F., Thomson N., et al. 2018a. Sensing Coated Iron-Oxide Nanoparticles with Spectral Induced Polarization (SIP): Experiments in Natural Sand Packed Flow-Through Columns. Environmental Science & Technology, 52(24), 14256-14265.

Mellage A., Smeaton C. M., Furman A., Atekwana E. A., Rezanezhad F., and Van Cappellen P. 2018b. Linking spectral induced polarization (SIP) and subsurface microbial processes: Results from sand column incubation experiments. Environmental Science & Technology, 52(4), 2081–2090.

Mitsch W., Gosselink J.G. 2015. Wetlands, 5th edition.

Mulcahy H., Charron-Mazenod L., and Lewenza S. 2008. Extracellular DNA chelates cations and induces antibiotic resistance in Pseudomonas aeruginosa biofilms. PLoS pathogens. 4(11), e1000213.

Nealson K. H. 2017. Bioelectricity (electromicrobiology) and sustainability. Microbial biotechnology, 10(5), 1114-1119.

Nicolotti G., Socco L.V., Martinis R., Godio A. and Sambuelli L. 2003. Application and comparison of three tomographic techniques for detection of decay in trees. Journal of Aboriculture, 29, 66-78.

Ntarlagiannis D., Williams K. H., Slater L., and Hubbard S. 2005. Low-frequency electrical response to microbial induced sulfide precipitation. Journal of Geophysical Research, 110(G2), 10.1029/2005JG000024.

Ntarlagiannis D., and Ferguson A. 2009. SIP response of artificial biofilms. Geophysics. 74(1), A1-A5.

Ntarlagiannis D., Robinson J., Soupios P., and Slater L. 2016. Field-scale electrical geophysics over an olive oil mill waste deposition site: Evaluating the information content of resistivity versus induced polarization (IP) images for delineating the spatial extent of organic contamination. Journal of Applied Geophysics, 135, 418–426. https://doi.org/10.1016/j.jappgeo.2016.01.017

Ntarlagiannis D., Ustra A., Kessouri P., and Flores-Orozco A. 2018. The Untapped Potential of the Induced Polarization Method: Characterizing and Monitoring Hydrocarbon Contamination in Soils. FastTimes, 23, 10.

Olsson P-I. 2018. Advances in time–domain induced polarization tomography: Data acquisition, processing and modelling. Ph.D. thesis, Department of Biomedical Engineering, Lund university.

Parker, N., Schneegurt, M., Tu, A.-H.T., Forster, B.M., Lister, P., 2016. Microbiology, Volume1. OpenStax College, American Society for Microbiology (https://openstax.org/details/books/microbiology). ISBN-13: 978-1-938168-14-7

Parnas H., 1975. Model for decomposition of organic material by microorganisms. Soil Biol. Biochem. 7, 161–169. https://doi.org/10.1016/0038-0717(75)90014-0

Personna Y.R., Ntarlagiannis D., Slater L. D., Yee N., O'Brien M., and Hubbard S. 2008. Spectral induced polarization and electrodic potential monitoring of microbially mediated iron sulfide transformation. Journal of Geophysical Research, 113(G2), 10.1029/2007JG000614

Personna Y. R., Slater L. D., Ntarlagiannis D., Werkema D., and Szabo Z. 2013a. Complex resistivity signatures of ethanol biodegradation in porous media. Journal of Contaminant Hydrology, 153, 37–50. https://doi.org/10.1016/j.jconhyd.2013.07.005

Personna Y. R., Slater L. D., Ntarlagiannis D., Werkema D., and Szabo Z. 2013b. Complex resistivity signatures of ethanol in sand-clay mixtures. Journal of Contaminant Hydrology, 149, 37–50. https://doi.org/10.1016/j.jconhyd.2013.03.005

Pester M., Knorr, K.-H., Friedrich, M.W., Wagner, M., Loy, A., 2012. Sulfate-reducing microorganisms in wetlands – fameless actors in carbon cycling and climate change. Front. Microbiol. 3, 72. https://doi.org/10.3389/fmicb.2012.00072

Piirto D.D. and Wilcox W.W. 1978. Critical Evaluation of the Pulsed-Current Resistance Meter for Detection of Decay in Wood. FPJ - Forest Product Journal, 28 (1), 52-57.

Pilon-Smits, E., 2005. PHYTOREMEDIATION. Annu. Rev. Plant Biol. 56, 15–39. https://doi.org/10.1146/annurev.arplant.56.032604.144214

Placencia-Gómez E., Slater L. D. Ntarlagiannis D., and Binley A. 2013. Laboratory SIP signatures associated with oxidation of disseminated metal sulfides. Journal of Contaminant Hydrology, 148, 25-38.

Ponziani M., Slob E. C., Vanhala H., and Ngan-Tillard D. J. M. 2012. Influence of physical and chemical properties on the low-frequency complex conductivity of peat. Near Surface Geophysics, 10(6), 491-501.

Poortinga A. T., Bos R., Norde W., and Busscher H. J. 2002. Electric double layer interactions in bacterial adhesion to surfaces. Surface science reports, 47(1), 1-32.

Postic F., and Doussan C. 2016. Benchmarking electrical methods for rapid estimation of root biomass. Plant Methods, 12(1), 33.

Prodan C., Mayo F., Claycomb J., Miller Jr J., and Benedik M. 2004. Low-frequency, low-field dielectric spectroscopy of living cell suspensions. Journal of Applied Physics. 95(7), 3754-3756.

Revil A., Schmutz M., and Batzle M. L. 2011. Influence of oil wettability upon spectral induced polarization of oil-bearing sands. Geophysics, 76(5), A31–A36. https://doi.org/10.1190/geo2011-0006.1

Revil A., Atekwana E., Zhang C., Jardani A., and Smith S. 2012. A new model for the spectral induced polarization signature of bacterial growth in porous media. Water Resources Research. 48(9), W09545.

Rosier C. L., Atekwana E. A., Aal G. A., and Patrauchan M. A. 2019. Cell concentrations and metabolites enhance the SIP response to biofilm matrix components. Journal of Applied Geophysics. 160, 183-194.

Salt D.E., Smith R.D., Raskin I., 1998. PHYTOREMEDIATION. Annu. Rev. Plant Physiol. Plant Mol. Biol. 49, 643–668. https://doi.org/10.1146/annurev.arplant.49.1.643

Sanchis A., Brown A., Sancho M., Martinez G., Sebastian J., Munoz S., and Miranda J. 2007. Dielectric characterization of bacterial cells using dielectrophoresis. Bioelectromagnetics: Journal of the Bioelectromagnetics Society, The Society for Physical Regulation in Biology and Medicine, The European Bioelectromagnetics Association. 28(5), 393-401.

Saneiyan S., Ntarlagiannis D., Werkema Colwell F. S., and Ohan J. 2016. Long Term Monitoring of Microbial Induced Soil Strengthening Processes. Abstract presented at the 49th annual Fall Meeting of the American Geophysical Union, San Francisco (USA), 12.12.2016 -13.12.2016.

Saneiyan S., Ntarlagiannis D., Werkema D. D. J., and Ustra A. 2018. Geophysical methods for monitoring soil stabilization processes. Journal of Applied Geophysics, 148, 234–244. https://doi.org/10.1016/j.jappgeo.2017.12.008

Saneiyan S., Ntarlagiannis D., Ohan J., Lee J., Colwell F., and Burns S. 2019. Induced polarization as a monitoring tool for in-situ microbial induced carbonate precipitation (MICP) processes. Ecological Engineering, 127, 36–47. https://doi.org/10.1016/j.ecoleng.2018.11.010

Sauck A.W., Atekwana E.A., Nash M.S., 1998. High electrical conductivities associated with an LNAPL plume imaged by integrated geophysical techniques. J. Environ. Eng. Geophys. 2, 203–212.

Schleifer N., Weller A., Schneider S. and JungeA. 2002. Investigation of a Bronze Age plankway by spectral induced polarization. Archaeological Prospection, 9(4), 243-253.

Schmutz M., Revil A., Vaudelet P., Batzle M., Viñao P. F., and Werkema D.D.J. 2010. Influence of oil saturation upon spectral induced polarization of oil-bearing sands. Geophysical Journal International, 183(1), 211–224. https://doi.org/10.1111/j.1365-246X.2010.04751.x

Schmutz M., Blondel A., and Revil A. 2012. Saturation dependence of the quadrature conductivity of oil-bearing sands. Geophysical Research Letters, 39(3), 2–7. https://doi.org/10.1029/2011GL050474

Schwan, H.P. 1957. Electrical Properties of Tissue and Cell Suspensions. Adv. Biol. Med. Phys. 5, 147–209. https://doi.org/10.1016/B978-1-4832-3111-2.50008-0.

Schwarz G. 1962. A theory of the low-frequency dielectric dispersion of colloidal particles in electrolyte solution1, 2. The Journal of Physical Chemistry. 66(12), 2636-2642.

Schwartz N., and Furman A. 2014. On the spectral induced polarization signature of soil organic matter. Geophysical Journal International, 200(1), 589-595.

Shigo A.L. and Shigo A. 1974. Detection of discoloration and decay in living trees and utility poles. Res. Pap. NE-294. Upper Darby, PA: U.S. Department of Agriculture, Forest Service, Northeastern Forest Experiment Station. 11p.

Slater L. D., and Lesmes D. 2002. IP Interpretation in Environmental Investigations. Geophysics, 67(1), 77–88. https://doi.org/10.1190/1.1451353.

Slater L. D., Ntarlagiannis D., Personna Y. R., and Hubbard S.S. 2007. Pore-scale spectral induced polarization signatures associated with FeS biomineral transformations. Geophysical Research Letters, 34, L21404.

Smith R. W., Fujita Y., Hubbard S. S., and Ginn T. R. 2012. Field Investigations of Microbially Facilitated Calcite Precipitation for Immobilization of Strontium-90 and Other Trace Metals in the Subsurface. Annu. Principal Investigators Meet., 4th, Lansdowne, VA, 20, 23. Final No. DE-FG02-07ER64404

Stamm A.J. 1930. An Electrical Conductivity Method for Determining the Moisture Content of Wood. Industrial and engineering chemistry, 19 (9), 1021-1025.

Stokes A., Atger C., Bengough A.G., Fourcaud T., Sidle R.C., 2009. Desirable plant root traits for protecting natural and engineered slopes against landslides. Plant Soil 324, 1–30. https://doi.org/10.1007/s11104-009-0159-y

Sumner J. S. 1976. Principles of Induced Polarization for Geophysical Exploration. Elsevier. https://www.sciencedirect.com/bookseries/developments-in-economic-geology/vol/5.

Swanson F.J., Dyrness C.T., 1975. Impact of clear-cutting and road construction on soil erosion by landslides in the western Cascade Range, Oregon. Geology 3, 393. https://doi.org/10.1130/0091-7613(1975)3<393:IOCARC>2.0.CO;2

Tinker P.B., Nye P.H., 2000. Solute movement in the rhizosphere. Oxford University Press.

Ustra A., Slater L. D., Ntarlagiannis D., and Elis V. 2012. Spectral Induced Polarization (SIP) signatures of clayey soils containing toluene. Near Surface Geophysics, 10(6), 503-515. https://doi.org/10.3997/1873-0604. 2012015

Ustra A., Mendonça C. A., Ntarlagiannis D., and Slater L. D. 2016. Relaxation Time Distribution Obtained from a Debye Decomposition of Spectral Induced Polarization Data. Geophysics, 81(2), E129–138. https://doi.org/10.1190/GEO2015-0095.1.

Vacheron J., Desbrosses G., Bouffaud,M.-L., Touraine B., Moënne-Loccoz Y., Muller D., Legendre L., Wisniewski-Dyé F., Prigent-Combaret C. 2013. Plant growth-promoting rhizobacteria and root system functioning. Front. Plant Sci. 4, 356. https://doi.org/10.3389/fpls.2013.00356.

Vanderborght J., Huisman J. A., van der Kruk J., and Vereecken H. 2013. Geophysical methods for field-scale imaging of root zone properties and processes. Soil-Water-Root Processes: Advances in

Tomography and Imaging. Editors: S.H. Anderson and J.W. Hopmans. SSSA Special Publication, 61, 247-282.

van Beem J., Smith M. E., and Zobel R. W. 1998. Estimating root mass in maize using a portable capacitance meter. Agronomy Journal 90(4), 566–570.

van der Wal A., Minor M., Norde W., Zehnder A. J., and Lyklema J. 1997a. Conductivity and dielectric dispersion of gram-positive bacterial cells. Journal of colloid and interface science, 186(1), 71-79.

van der Wal A., Minor M., Norde W., Zehnder A. J., and Lyklema J. 1997b. Electrokinetic potential of bacterial cells, Langmuir. 13(2), 165-171.

Vanhala H. 1997. Laboratory and field studies of environmental and exploration applications of the spectral induced-polarization (SIP) method : Doctoral Thesis, Synopsis. Retrieved from http://arkisto.gtk.fi/ej/ej22.pdf

Vinegar H. J., and Waxman M. H. 1984. Induced polarization of shaly sands, 49(8), 1267–1287.

Vives-Rego J., Lebaron P., and Nebe-von Caron G. 2000. Current and future applications of flow cytometry in aquatic microbiology. FEMS Microbiology Reviews, 24(4), 429-448.

Walter J., Lück E., Bauriegel A., Richter C., and Zeitz J. 2015. Multi-scale analysis of electrical conductivity of peatlands for the assessment of peat properties. European journal of soil science, 66(4), 639-650.

Wang P, Kinraide T. B., Zhou D., Kopittke P. M., and Peijnenburg W.J.G.M. 2011. Plasma membrane surface potential: Dual effects upon ion uptake and toxicity. Plant Physiology, 155(2), 808-820.

Wang B., Mezlini A. M., Demir F., Fiume M., Tu Z., Brudno M., et al. 2014. Similarity network fusion for aggregating data types on a genomic scale. Nature Methods, 11(3), 333.

Wanjari S., Prabhu C., Yadav R., Satyanarayana T., Labhsetwar N., and Rayalu S. 2011. Immobilization of carbonic anhydrase on chitosan beads for enhanced carbonation reaction. Process Biochemistry, 46(4), 1010–1018. https://doi.org/10.1016/j.procbio.2011.01.023

Ward S. H. 1980. Electrical, Electromagnetic, and Magnetotelluric Methods. Geophysics, 45(11), 1659–1666. https://doi.org/10.1190/1.1441056.

Wardman C., Nevin K. P., and Lovley D. R. 2014. Real-time monitoring of subsurface microbial metabolism with graphite electrodes. Frontiers in Microbiology. 5, 621.

Weigand M. 2017. Monitoring structural and physiological properties of crop roots using spectral electrical impedance tomography, Ph.D. thesis, University of Bonn, doi:10.5281/zenodo.400833.

Weigand M., and Kemna A. 2016. Relationship between Cole–Cole Model Parameters and Spectral Decomposition Parameters Derived from SIP Data. Geophysical Journal International, 205(3). 1414–1419. doi: 10.1093/gji/ggw099.

Weigand M. and Kemna A. 2017. Multi-frequency electrical impedance tomography as a non-invasive tool to characterize and monitor crop root systems. Biogeosciences, 14(4), 921–939. doi: 10.5194/bg-14-921-2017

Weigand M. and Kemna A. 2019. Imaging and functional characterization of crop root systems using spectroscopic electrical impedance measurements, Plant and Soil, 435(1-2), 201-224. doi:10.1007/s11104-018-3867-3.

Weihs U., Dubbel V., Krummheuer F. and Just A. 1999. Die elektrische Widerstandstomographie, Forst und Holz, 54, 166-170.

Whitchurch C. B., Tolker-Nielsen T., Ragas P. C., and Mattick J. S. 2002. Extracellular DNA required for bacterial biofilm formation. Science. 295(5559), 1487-1487.

Willey, J.M., Sherwood, L., Woolverton, C.J., 2014. Prescott's microbiology, Ninth edition. ed. McGraw-Hill, New York, NY. ISBN-13: 978-0073402406

Williams K. H., Ntarlagiannis D., Slater L. D., Dohnalkova A., Hubbard S. S., Banfield J. F. 2005. Geophysical imaging of stimulated microbial biomineralization, Environmental Science and Technology, 39(19), 7592-7600.

Williams K. H., Kemna A., Wilkins M. J., Druhan J., Arntzen E., N'Guessan A. L., Long P. E., Hubbard S. S., and Banfield J. F. 2009, Geophysical monitoring of coupled microbial and geochemical processes during stimulated subsurface bioremediation. Environmental science & technology, 43(17), 6717-6723. doi:10.1021/es900855j

Wong J. 1979. An electrochemical model of the induced-polarization phenomenon in disseminated sulfide ores. Geophysics, 44(7), 1245-1265.

Wu Y., Slater L. D., Versteeg R., and LaBrecque D. 2008. A comparison of the low frequency electrical signatures of iron oxide versus calcite precipitation in granular zero valent iron columns. Journal of Contaminant Hydrology, 95(3-4), 154–67. https://doi.org/10.1016/j.jconhyd.2007.09.003

Wu Y., Versteeg R., Slater L., and LaBrecque D. 2009. Calcite precipitation dominates the electrical signatures of zero valent iron columns under simulated field conditions. Journal of Contaminant Hydrology, 106(3-4), 131–43. https://doi.org/10.1016/j.jconhyd.2009.02.003

Wu Y., Hubbard S. S., Williams K. H. and Ajo-Franklin J. 2010. On the complex conductivity signatures of calcite precipitation. Journal of Geophysical Research: Biogeosciences, 115, no. G2. doi:10.1029/2009JG001129.

Wu Y., Ajo-Franklin J.B., Spycher N., Hubbard S. S., Zhang G., Williams K. H., Taylor J., et al. 2011. Geophysical monitoring and reactive transport modeling of ureolytically-driven calcium carbonate precipitation. Geochem. Trans., 12, 1–20. doi:10.1186/1467-4866-12-7

Wu Y., Surasani V. K., Li L., and Hubbard S. S. 2014. Geophysical monitoring and reactive transport simulations of bioclogging processes induced by Leuconostoc mesenteroides Bioclogging monitoring and simulation. Geophysics, 79(1), E61-E73.

Yadav R., Labhsetwar N., Kotwal S., and Rayalu S. 2011. Single enzyme nanoparticle for biomimetic CO2 sequestration. Journal of Nanoparticle Research, 13(1), 263–271. https://doi.org/10.1007/s11051-010-0026-z

Zarif F., Kessouri P. and Slater L. D. 2017. Recommendations for field-scale Induced Polarization (IP) data acquisition and interpretation. Journal of Environmental and Engineering Geophysics, 22(4), 395-410. doi:10.2113/JEEG22.4.395

Zhang C., Slater L. D., Redden G., Fujita Y., Johnson T., and Fox D. 2012. Spectral induced polarization signatures of hydroxyl adsorption in porous media. Environmental Science & Technology, 46(8), 4357-4364.

Zhang C., Revil A., Fujita Y., Munakata-Marr J., and Redden G. 2014. Quadrature conductivity: A quantitative indicator of bacterial abundance in porous media. Geophysics, 79(6), D363-D375.

Zhao Y., Zimmermann E., Huisman J. A., Treichel A., Wolters B., van Waasen S., and Kemna A. 2015. Phase corrections of electromagnetic coupling effects in cross-borehole EIT measurements. Measurement Science and Technology, 26(1), 15801.

Zhao Y., Zimmermann E., Huisman J. A., Treichel A., Wolters B., van Waassen S., and Kemna A. 2013. Broadband EIT borehole measurements with high phase accuracy using numerical corrections of electromagnetic coupling effects. Measurement Science and Technology, 24(8), 085005.

Zimmermann E., Huisman J.A., Mester A., and van Waasen S. 2019. Correction of phase errors due to leakage currents in wideband field EIT measurements on soil and sediments. Measurement Science and Technology, 30, 084002.

Zürcher E. 1988. Diagnosemethode des Gesundheits und Vitalitätszustandes der Bäume. Vierteljahresschr. Naturforsch. Ges. Zürich, 133 (1), 25-42.